

RNA Sequencing Analysis of the Broad-Host-Range Strain *Sinorhizobium fredii* NGR234 Identifies a Large Set of Genes Linked to Quorum Sensing-Dependent Regulation in the Background of a *traI* and *ngrI* Deletion Mutant

Dagmar Krysciak,^a Jessica Grote,^a Mariita Rodriguez Orbegoso,^a Christian Utpatel,^a Konrad U. Förstner,^b Lei Li,^{b,c} Christel Schmeisser,^a Hari B. Krishnan,^d Wolfgang R. Streit^a

Biozentrum Klein Flottbek, Abteilung für Mikrobiologie und Biotechnologie, Universität Hamburg, Hamburg, Germany^a; Core Unit Systems Medicine, Universität Würzburg, Würzburg, Germany^b; Institut für Molekulare Infektionsbiologie, Universität Würzburg, Würzburg, Germany^c; Plant Genetics Research Unit, United States Department of Agriculture-Agricultural Research Service, University of Missouri, Columbia, Missouri, USA^d

The alphaproteobacterium *Sinorhizobium fredii* NGR234 has an exceptionally wide host range, as it forms nitrogen-fixing nodules with more legumes than any other known microsymbiont. Within its 6.9-Mbp genome, it encodes two *N*-acyl-homoserine-lactone synthase genes (i.e., *traI* and *ngrI*) involved in the biosynthesis of two distinct autoinducer I-type molecules. Here, we report on the construction of an NGR234- Δ *traI* and an NGR234- Δ *ngrI* mutant and their genome-wide transcriptome analysis. A high-resolution RNA sequencing (RNA-seq) analysis of early-stationary-phase cultures in the NGR234- Δ *traI* background suggested that up to 316 genes were differentially expressed in the NGR234- Δ *traI* mutant versus the parent strain. Similarly, in the background of NGR234- Δ *ngrI* 466 differentially regulated genes were identified. Accordingly, a common set of 186 genes was regulated by the TraI/R and NgrI/R regulon. Coregulated genes included 42 flagellar biosynthesis genes and 22 genes linked to exopolysaccharide (EPS) biosynthesis. Among the genes and open reading frames (ORFs) that were differentially regulated in NGR234- Δ *traI* were those linked to replication of the pNGR234*a* symbiotic plasmid and cytochrome *c* oxidases. Biotin and pyrroloquinoline quinone biosynthesis genes were differentially expressed in the NGR234- Δ *ngrI* mutant as well as the entire cluster of 21 genes linked to assembly of the NGR234 type III secretion system (T3SS-II). Further, we also discovered that genes responsible for rhizopine catabolism in NGR234 were strongly repressed in the presence of high levels of *N*-acyl-homoserine-lactones. Together with nodulation assays, the RNA-seq-based findings suggested that quorum sensing (QS)-dependent gene regulation appears to be of higher relevance during nonsymbiotic growth rather than for life within root nodules.

The ability of bacteria to sense a certain population density has become known as quorum sensing (QS). Quorum sensing is a cell density-dependent system of gene regulation in prokaryotes (1, 2). Through the accumulation of bacterially produced signaling molecules (autoinducers [AIs]), the bacterial population is able to sense increases in cell density and alter gene expression accordingly. Many examples of QS-dependent gene regulation processes have been described in a wide variety of Gram-negative and Gram-positive species. Thereby, it was found that pathogenicity, biofilm formation, production of extracellular proteins, secondary metabolite production, and other processes are often subject to QS-dependent regulation. *N*-Acyl-homoserine-lactones (AHLs) are the key signaling molecules in the cell density-dependent system of gene regulation in many Gram-negative bacteria (3, 4). The AHLs are synthesized through a LuxI-like protein (EC 2.3.1.184), using *S*-adenosylmethionine (SAM) and an acyl-acyl carrier protein (acyl-ACP) from the fatty acid biosynthesis pathway (5). Within the cells, the signals are recognized by the LuxR-type receptor/regulator proteins (6), building up complexes that subsequently stimulate subordinated processes.

Many soil bacteria interact with plants in ways that range from symbiotic and beneficial to pathogenic associations. Some symbiotic alpha- and betaproteobacteria (commonly called rhizobia) are able to form nitrogen-fixing root nodules together with the legume plant. The symbiosis is initiated by a signal exchange between the legume plant and the microbe (7–9). Within this frame-

work, it is noteworthy that some rhizobia have evolved mechanisms that allow them to nodulate a larger variety of legume plants than others. These strains have been designated “broad-host-range” strains, and they are promiscuous with respect to the selection of their host plants (10). *Sinorhizobium fredii* NGR234 (here called NGR234) nodulates more than 120 genera of legumes and the nonlegume *Parasponia andersonii* (10, 11). No other strain with such a wide host range is currently known, and mainly because of its host range, NGR234 is a well-studied model organism. NGR234 was isolated in 1965 from the lablab bean (*Lablab purpureus*) in Papua New Guinea (12). Its 6.9-Mbp genome encodes a remarkable number of secretion systems and other interesting features that give some clues to the molecular keys to broad host range (13 and references therein).

The NGR234 genome encodes two distinct QS systems where

Received 3 June 2014 Accepted 30 June 2014

Published ahead of print 7 July 2014

Editor: C. R. Lovell

Address correspondence to Wolfgang R. Streit, wolfgang.streit@uni-hamburg.de.

Supplemental material for this article may be found at <http://dx.doi.org/10.1128/AEM.01835-14>.

Copyright © 2014, American Society for Microbiology. All Rights Reserved.

doi:10.1128/AEM.01835-14

TABLE 1 Primers used in this study to construct and verify NGR234- Δ *traI*, NGR234- Δ *ngrI*, and NGR234- Δ *ngrI*/ Δ *traI* deletion and NGR234-c Δ *traI* and NGR234-c Δ *ngrI* complementation mutant strains

Oligonucleotide	Sequence 5'–3' ^a	Size (bp)	Target region/description
traI_–500_for	<u>GAATTC</u> TCGAGTTCTGAGTTGCTGCGG	27	5' region of <i>traI</i>
traI_–500_rev	TCTAGAGAATTCTCCGTCGTTGTTG	26	
traI_+500_rev	CTGCAGCTGCATTTGCGAGCGTCGTT	26	3' region of <i>traI</i>
traI_+500_for	TCTAGAGGAGAAATCAGTGGAACAGC	26	
GmR_F_XbaI	GACATCTAGAGACGCACACCGTGAAAC	28	Gm ^r cassette
GmR_R_XbaI	TAATCTAGACCGCGATCATCAAGGCCGTG	29	
ngrI_A_for	GCGAATTCTGCTGGCGATCAGTGCCAAC	28	5' region of <i>ngrI</i>
ngrI_A_rev	GCTCTAGACGGTCTTGACGTCCCATTTC	28	
ngrI_B_for	GCTCTAGAATCGCTGGGAAGTATCGAG	28	3' region of <i>ngrI</i>
ngrI_B_rev	GCCTGCAGGAAACCGCGCGGTGAAATC	28	
traI_del_for	CAACGTCACCGCGAAATAG	19	External control primers
traI_del_rev	TCGCTGGTACGAAGAAGAAC	20	
traI_frag_for	GACGATCTTCAACCGACCTAC	21	Internal control primers
traI_frag_rev	GGAGCCTCATGAATGTGTCTG	21	

^a Inserted restriction sites are underlined.

one of the AI synthases is designated *traI* and the second gene is designated *ngrI*. TraI synthesizes an AHL that is *N*-(3-oxooctanoyl)-L-homoserine lactone (here called 3-oxo-C₈-HSL) (14), and *ngrI* encodes an enzyme that probably synthesizes a not-yet-characterized derivative of an autoinducer I-type molecule (13). TraI is encoded on the 0.54-Mbp symbiotic replicon pNGR234a as part of a conserved cluster of genes that share a high degree of synteny with the Ti plasmid of *Agrobacterium tumefaciens* (13, 14). This conserved cluster contains, beside the *traI* gene, the *traR* and *traM* regulatory genes as well as other genes required for conjugative DNA transfer and replication of the plasmid. With respect to the high synteny with *A. tumefaciens*, it can be postulated that TraR associates with 3-oxo-C₈-HSL and that it is involved in transcriptional activation of QS-dependent promoters (14). TraM is a homolog of the corresponding antiactivator protein in *A. tumefaciens*, preventing TraR from activating the target genes in the presence of low levels of AIs. Furthermore, NgrI is encoded on the NGR234 chromosome together with its cognate receptor/regulator protein NgrR. NgrI is a functional homolog of *Sinorhizobium meliloti* SinI. However, the *sinI* gene is involved in the synthesis of several long-chain AHLs ranging from 12 to 18 carbons in length (15). The SinI/SinR- and ExpR-dependent gene regulation has been intensively characterized in this model organism (16–21); thereby, the different researchers have outlined a very complex and partially strain-specific regulatory network in this narrow-host-range strain.

Recently, high-resolution transcriptome studies using RNA sequencing (RNA-seq) technologies have given us a very detailed and reliable insight into expression profiles of many model organisms (22–25). However, only a few studies so far have used this technology for the genome-wide analysis of QS-dependent expression profiles. The focus of these studies was on the opportunistic pathogenic microorganism *Burkholderia cenocepacia* (26) and on *Pseudomonas aeruginosa* (27, 28). Interestingly, no study has yet focused on the QS-dependent gene regulation in sinorhizobia or closely related species using RNA-seq. Only very recently, an RNA-seq analysis was published on NGR234 with respect to a genome-wide change of the expression profile of the symbiotic lifestyle in bacteroids of two legume plants (29). This study has already given us a very detailed insight into the complexity of many processes linked to the bacterial infection process.

In the current study, high-resolution RNA-seq was used to analyze the expression profile of the NGR234 wild-type strain compared to newly constructed NGR234- Δ *traI* and NGR234- Δ *ngrI* deletion mutants. The focus of the study was thus on the identification of QS-regulated genes. Our data suggested that a common set of 186 genes is QS regulated. Further RNA-seq data generated in early exponential phase and by challenging NGR234 with moderate and high levels of AI suggested that QS plays only a minor role during the onset of growth but that it has profound effects on motility, vitamin biosynthesis, secretion, and other key features of the organism during the stationary phase.

MATERIALS AND METHODS

Bacterial strains and growth conditions. *Sinorhizobium fredii* NGR234 was grown at 30°C in liquid TY medium (0.5% tryptone, 0.25% yeast extract, 10 mM CaCl₂, pH 7.0) at 200 rpm and supplemented with rifampin (25 µg/ml). NGR234 QS deletion mutants were cultivated under the same conditions as those for the NGR234 wild-type strain in TY medium which was additionally supplemented with gentamicin (10 µg/ml), and complemented NGR234 QS mutant strains were cultivated in TY medium supplemented with kanamycin (25 µg/ml). *Escherichia coli* was grown at 37°C on LB medium supplemented with the appropriate antibiotics. *Agrobacterium tumefaciens* NTL4 (30), carrying a *traI::lacZ* promoter fusion, was grown at 28°C in AT medium (31) containing 0.5% glucose per liter and supplemented with spectinomycin (50 µg/ml) and tetracycline (4.5 µg/ml). For sedimentation assays, the NGR234 parent strain as well as the constructed mutant strains was grown at 30°C and 200 rpm in 5 ml TY medium supplemented with appropriate antibiotics for 48 h. Then, cells were allowed to sediment at room temperature for up to 24 h without shaking.

Construction of NGR234 AI synthase mutants. Molecular cloning steps were in general done as outlined in reference 32, and mutant strains NGR234- Δ *traI* and NGR234- Δ *ngrI* were constructed as previously described (33). For the construction of a deletion mutant in the *traI* gene, an ~2.0-kb PCR fragment containing the 486-bp upstream region of *traI*, a 986-bp gentamicin resistance gene, and a 500-bp downstream fragment flanking the *traI* gene was cloned in the suicide vector pNPTS138-R6KT (34). For this purpose, the different PCR fragments were amplified from genomic DNA of NGR234 using primers as indicated in Table 1. The gentamicin gene was derived from the broad-host-range cloning vector pBBR1MCS-5 (35). The resulting construct (pNPTS138-*traI::gm*) was transformed into NGR234 by conjugation. Single recombinant clones carrying this construct were selected on TY medium containing gentamicin and rifampin. To obtain double recombinant mutants, bacteria were

TABLE 2 Overall transcriptome statistics for the 12 analyzed NGR234 samples^a

Sample no.	Treatment	NGR234 genotype	Growth phase/OD ₆₀₀	3-Oxo-C ₈ -HSL added	No. of reads generated (10 ⁶)	No. of uniquely mapped reads (10 ⁶)
1	A	wt	Stationary/3.26	None	7.15	3.55
2	A	wt	Stationary/3.37	None	6.79	3.34
3	B	$\Delta traI$	Stationary/3.08	None	6.39	3.24
4	B	$\Delta traI$	Stationary/3.10	None	8.07	4.06
5	C	$\Delta ngrI$	Stationary/3.30	None	6.79	3.62
6	C	$\Delta ngrI$	Stationary/3.24	None	7.82	4.37
7	D	wt	Exponential/0.22	None	4.35	1.51
8	D	wt	Exponential/0.22	None	8.74	2.83
9	E	wt	Exponential/0.26	0.05 μ M	8.04	1.58
10	E	wt	Exponential/0.27	0.05 μ M	6.68	1.41
11	F	wt	Exponential/0.22	50 μ M	3.86	1.77
12	F	wt	Exponential/0.21	50 μ M	9.16	2.73

^a “Stationary” indicates cultures grown to early stationary phase; “Exponential” indicates cultures grown to early exponential phase (see Fig. S1 in the supplemental material). Cultures 1 to 6 were harvested after 34 to 40 h of growth. Cultures 7 to 12 were harvested after 3 h upon addition of 3-oxo-C₈-HSL. Controls were supplemented with an equal amount of ethyl acetate. Two cultures represent one treatment (experiment). wt, wild type, NGR234 parent strain; $\Delta traI$, NGR234- $\Delta traI$ mutant strain; $\Delta ngrI$, NGR234- $\Delta ngrI$ mutant strain.

streaked on the same medium (lacking the antibiotics) in the presence of 10% sucrose. In our deletion mutant, the entire *traI* gene was deleted starting from the ATG to the last codon of the gene. The *ngrI* mutant strain was generated as described above using an ~2.1-kb EcoRI-PstI fragment containing the flanking regions of *ngrI* and the same gentamicin resistance gene. Thereby, the majority of the *ngrI* gene (645 bp) ranging from bp 116 to bp 534 was deleted. The obtained mutations were verified by PCR using different primer pairs flanking the *traI* and *ngrI* genes (Table 1) and by sequencing.

For complementation of the above-constructed QS mutants, the wild-type *traI* and *ngrI* genes, including promoter regions, were amplified using individual flanking primer pairs (Table 1), inserted into pBBR1MCS-2 (35), and reintroduced by conjugation into the respective mutant strain NGR234- $\Delta traI$ or NGR234- $\Delta ngrI$. Recombinant NGR234 QS mutant clones carrying the construct were selected on TY medium containing kanamycin and rifampin and designated NGR234-c $\Delta traI$ and NGR234-c $\Delta ngrI$, respectively. The correctness of the complemented mutant strains was verified by PCR.

Furthermore, to study the importance of the AIs for rhizosphere colonization of NGR234, a double QS mutant designated NGR234- $\Delta ngrI/\Delta traI$ having a deletion in both the *traI* and *ngrI* loci was generated. The construction of the double mutant was based on the NGR234- $\Delta ngrI$ deletion mutant in which the *traI* locus was deleted as described above. The double QS mutant was verified by PCR and sequencing.

TLC coupled with *A. tumefaciens* soft agar overlay assay. Separation of AI molecules produced by the NGR234 parent and the above-constructed mutant strains was carried out using thin-layer chromatography (TLC) and by using the *A. tumefaciens* reporter strain NTL4 (30). Therefore, AIs were extracted from stationary-phase cultures with an equal volume of ethyl acetate. The extraction was carried out twice. Pooled extracts were concentrated *in vacuo* and resuspended in 1 ml ethyl acetate. Sample volumes of 1 to 10 μ l were applied to cellulose TLC plates (Polygram Cel MN300 AC-30; Macherey-Nagel, Düren, Germany), developed with methanol-water (60:40, vol/vol), and air dried. Detection of AIs was carried out according to the method of Zhu et al. (36) by overlaying the TLC plates with *A. tumefaciens* soft agar containing *A. tumefaciens* NTL4. A 10⁻⁸ M solution of 3-oxo-C₈-HSL and a 10⁻⁶ M solution of *N*-(3-oxododecanoyl)-L-homoserine lactone (Sigma-Aldrich, Heidelberg, Germany) were prepared in ethyl acetate and used as standards. Overlaid TLC plates were incubated overnight at 30°C.

Preparation of transcriptome samples. The different NGR234 cultures used in this study for a transcriptome analysis are summarized in Table 2. Prior to cultivation of large 200-ml cultures, precultures were established from cryocultures in 5 ml TY medium and cultivated at 30°C

and 200 rpm. For the transcriptome analyses of early-stationary-growth-phase cultures, 200 ml TY medium was inoculated with freshly grown precultures of NGR234 wild type as well as the mutant strains and cultivated for approximately 34 to 40 h at 30°C and 200 rpm as batch cultures (Table 2, samples 1 to 6, treatments A to C). After reaching an optical density at 600 nm (OD₆₀₀) of 3.1 to 3.3, cultures were separated into fractions of 50 ml, which were then transferred into Falcon tubes containing 10 ml ethanol-phenol (95:5). Samples were mixed well, directly frozen in liquid nitrogen, and stored at -70°C until further use. For transcriptome analyses of early-exponential-growth-phase cultures, 200 ml TY medium was inoculated with a freshly grown preculture of NGR234 wild type and cultivated at 30°C and 200 rpm till it reached an OD₆₀₀ of 0.1 (Table 2, samples 7 to 12, treatments D to F). Cultures were then divided into two separate fractions of 100 ml of which one was supplemented with either 0.05 μ M or 50 μ M 3-oxo-C₈-HSL (stock solution of 3-oxo-C₈-HSL was prepared in ethyl acetate) and the other culture fraction (control) was treated with an equal aliquot of ethyl acetate. Cultures were allowed to grow for 3 additional hours and then harvested into Falcon tubes and treated as outlined above.

RNA extraction, library construction, sequencing, and bioinformatic analysis of transcriptome samples. For all NGR234 wild-type and mutant strains, RNA-seq libraries were constructed from independent biological duplicates of RNA samples. Six samples were harvested at the early exponential phase, and six samples were obtained from stationary-growth-phase cultures (Table 2; see also Fig. S1 in the supplemental material). Total RNA was extracted using the hot-phenol method described previously (37). The residual genomic DNA was removed from the total isolated RNA by DNase I treatment. The cDNA libraries for sequencing were constructed by Vertis Biotechnology AG, Germany, as described by Sharma et al. (24). The transcripts were not fragmented in order to get mainly sequencing reads of the 5' end of the transcripts. The obtained cDNA libraries were sequenced using a HiSeq 2500 machine (Illumina) in single-read mode and running 100 cycles. For the 12 analyzed samples, we sequenced between 3.86 and 9.16 million cDNA reads. The bioinformatic analysis was done as described in the work of Dugar et al. (38). To ensure a high sequence quality, the Illumina reads in FASTQ format were trimmed with a cutoff phred score of 20 by the program fastq_quality_trimmer from FASTX-Toolkit version 0.0.13 (http://hannonlab.cshl.edu/fastx_toolkit/). The alignment of reads, coverage calculation, gene-wise read quantification, and differential gene expression were performed with READemption (K. U. Förstner, J. Vogel, and C. M. Sharma, posted on bioRxiv under doi:10.1101/003723) which was relying on ‘segemehl’ version X (39) and DESeq version V. Visual inspection of the coverages was done using the Integrated Genome Browser (IGB) (40). The reference

TABLE 3 Gene-specific primers used for qRT-PCR

Oligonucleotide	Sequence, 5'–3'	Size (bp)	Target gene/ORF
RT_rpoD_for	ACATCACCAATGTCGGCGGTGAAG	162	<i>rpoD</i>
RT_rpoD_rev	TGCAGCTTGC GGAGCTTCTTGTAG		
RT_flgB_for	AGAATGTCGTGGCCGGCAACATC	238	<i>flgB</i>
RT_flgB_rev	GCCCGTCTTCATCATTCTCTGCTC		
RT_pilA_for	ACCATTTTCGCCCGCCTGATGAAG	172	<i>pilA</i>
RT_pilA_rev	ATGTTGGTTTCGGCGGTCGTCATCT		
RT_b22870_for	CCTCTGACGCTCGATGTCCTGAA	110	NGR_b22870
RT_b22870_rev	GTCGCTGAGCATCAGGTCGCAAT		
RT_exoI_for	CGATGGCGACACCATCGAAATTGC	257	<i>exoI</i>
RT_exoI_rev	GATTC AACCATCCAGCGGTTGACG		
RT_c14830_for	CGGGTTGCTGCATATGTATCGACCT	220	NGR_c14830
RT_c14830_rev	GGCCTGATACTCTTCGATCAGCATC		

sequences and gene annotations for NGR234 were retrieved from the NCBI database (accession numbers: pNGR234a, NC_000914.2; pNGR234b, NC_012586.1; cNGR234, NC_012587.1) and in part manually reannotated. Genes with a fold change of ≥ 2.0 and an adjusted *P* value (*P* value was corrected by false discovery rate [FDR] based on the Benjamini-Hochberg procedure) of ≤ 0.05 were considered differentially expressed.

qRT-PCR. Quantitative RT-PCR (qRT-PCR) experiments were carried out to verify selected QS-regulated genes. Total RNA was extracted from stationary-phase-grown cultures according to the method of Rivas et al. (41), and the residual genomic DNA was removed by DNase I treatment according to the manufacturer's instructions (DNase I, RNase-free; Thermo Scientific, WI, USA). The SuperScript VILO cDNA synthesis kit (Invitrogen, Life Technologies, TX, USA) was used to generate cDNA using 1.9 μ g RNA. Gene-specific primers used for qRT-PCR are shown in Table 3. The qRT-PCRs were set up according to the manufacturer's protocol using the SYBR Select master mix for CFX (Applied Biosystems by Life Technologies, TX, USA) and performed in the MiniOpticon real-time PCR detection system (Bio-Rad Laboratories, Munich, Germany). Standard curves of 10-fold serial dilutions of cDNA were generated for each gene to evaluate the primer efficiency and for data analysis. The efficiency, slope, and correlation coefficient were determined by the CFX Manager software (Bio-Rad Laboratories, Munich, Germany). All qRT-PCRs were run in triplicate and repeated at least three times in separate experiments under the same conditions. To normalize variability in expression levels, *rpoD* was used as the internal control gene. Data were analyzed based on the normalized gene expression (threshold cycle [$2^{-\Delta\Delta CT}$] method) and the above-stated software.

Nodulation assays. Nodulation assays accomplished with NGR234- $\Delta traI$, NGR234- $\Delta ngrI$, and NGR234- $\Delta ngrI/\Delta traI$ and with *Vigna unguiculata*, *Vigna radiata*, and *Tephrosia vogelii* were done as previously described (42). Experiments were repeated two times with five plants per treatment in each experiment. Plants were harvested 30 days after inoculation. Nodules formed on the roots were counted, and the shoot fresh weight was recorded. Plants grown in the absence of rhizobia were used as a control.

Microarray data accession number. The raw, demultiplexed reads as well as coverage files have been deposited in the National Center for Biotechnology Information's Gene Expression Omnibus (43) under the accession number GSE54381.

RESULTS AND DISCUSSION

Construction and phenotype analysis of *traI* and *ngriI* deletion mutants. To investigate the QS-mediated gene regulation in the broad-host-range strain *Sinorhizobium fredii* NGR234, we followed several strategies. First, we constructed an NGR234- $\Delta traI$, an NGR234- $\Delta ngrI$, and an NGR234- $\Delta ngrI/\Delta traI$ deletion mutant and analyzed their AI profile using TLC separation with subse-

quent AI detection by *A. tumefaciens* NTL4 (36). While we repeatedly detected two spots in extracts of the NGR234 parent strain, we detected only a single spot in the NGR234- $\Delta traI$ and the NGR234- $\Delta ngrI$ mutant strains. No AI was detected in extracts obtained from the double mutant. However, complemented strains NGR234-c $\Delta traI$ and NGR234-c $\Delta ngrI$ produced again high levels of the respective AI molecules (see Fig. S2 in the supplemental material). The observation of two AI molecules in the parent strain and one AI in each of the single-knockout mutant strains corresponds well with previous results (13, 14).

Since it is well known that the lack of AI molecules can have profound effects on motility and exopolysaccharide (EPS) production, we analyzed our mutants for possible phenotypes. Interestingly, we did not observe reproducible motility phenotypes on solid media and using swimming and swarming agar (data not shown). Also, growing NGR234 mutant cells on medium containing Congo red or calcofluor white did not produce stable phenotypes. However, analyzing motility in liquid TY medium resulted in the observation of strong sedimentation phenotypes for the mutants (Fig. 1). Thus, parent strain cultures settled within 3 to 24 h, while the mutant strains did not sediment. The observed sedimentation phenotype for NGR234- $\Delta ngrI$ was completely restored using the NGR234-c $\Delta ngrI$ strain. The phenotype produced by NGR234- $\Delta traI$ could be only partially recovered by adding the parental gene back into NGR234- $\Delta traI$ (Fig. 1). Further tests and chemical complementation using a micromolar concentration of 3-oxo-C₈-HSL produced similar results (data not shown). Therefore, it is likely that the sedimentation phenotype was mainly a



FIG 1 Sedimentation of NGR234 in TY medium. The NGR234 wild type (wt) shows a clear sedimentation phenotype in liquid TY medium after 3 to 24 h of incubation at room temperature without shaking, whereas $\Delta traI$ (NGR234- $\Delta traI$), $\Delta ngrI$ (NGR234- $\Delta ngrI$), and $\Delta ngrI/\Delta traI$ (NGR234- $\Delta ngrI/\Delta traI$) strains did not settle even after 24 h of incubation under the same conditions. The NGR234-c $\Delta ngrI$ (c $\Delta ngrI$) strain carries extra copies of the *ngriI* wild-type gene in the background of NGR234- $\Delta ngrI$ and was completely recovered; NGR234-c $\Delta traI$ (c $\Delta traI$) was partially recovered by adding extra copies of the wild-type gene into the NGR234- $\Delta traI$ mutant strain.

TABLE 4 Number of genes significantly altered in their expression profile in the NGR234 QS deletion mutants (early stationary phase) and in NGR234 after addition of 3-oxo-C₈-HSL at two different concentrations (early exponential phase)^a

NGR234 genotype ^c	Growth phase/treatment	Total no. of differentially expressed genes ^b	No. of differentially expressed genes on replicons (cNGR234/pNGR234b/pNGR234a)
$\Delta traI$	Stationary	316	221/82/13
$\Delta ngrI$	Stationary	466	303/155/8
wt	Exponential; 0.05 μ M 3-oxo-C ₈ -HSL added	13	8/3/2
wt	Exponential; 50 μ M 3-oxo-C ₈ -HSL added	4	0/4/0

^a Data are mean values of two independent treatments.

^b Total number of significantly, differentially expressed genes having a fold change of ≥ 2.0 and an adjusted *P* value of ≤ 0.05 .

^c wt, wild type, NGR234 parent strain; $\Delta traI$, NGR234- $\Delta traI$ mutant strain; $\Delta ngrI$, NGR234- $\Delta ngrI$ mutant strain.

result of a strong upregulation of the flagellar gene expression and thus a motility phenotype. Altogether, these findings confirmed the importance of the *traI* and *ngrI* genes for biofilm formation, sedimentation, and motility, and they suggested that the observed phenotypes are mainly caused by the deletion of the respective AI synthase gene.

Global pattern of QS-dependent gene expression in NGR234.

In a parallel approach, we examined the global gene expression pattern of the wild type and its two AI synthase mutants (NGR234- $\Delta traI$ and NGR234- $\Delta ngrI$) by comparing their transcriptome profile at the early stationary growth phase to those of the NGR234 wild type and each other. We chose this time point because it can be expected that during the onset of stationary growth phase many QS-dependent processes are turned on. For these experiments, cells were grown for approximately 40 h to a final OD₆₀₀ not greater than 3.4 prior to total RNA extraction. The NGR234 parent strain was cultivated like the control for the same time period to an identical OD₆₀₀ and then treated equally (Table 2).

Further, we analyzed the short-term response of the parent strain to externally added 3-oxo-C₈-HSL in the early exponential growth phase. For this, cells were grown to an OD₆₀₀ of 0.1 and then challenged by the presence of a moderate (0.05 μ M) and a high (50 μ M) concentration of 3-oxo-C₈-HSL. Total RNA was already extracted after 3 h from the AHL-induced samples and the control cultures. The OD₆₀₀ of these exponentially growing cultures at the time of harvest was 0.24 (± 0.03) (Table 2).

For all samples, the cDNA libraries were constructed and sequenced as described in Materials and Methods. For each of the six treatments, two independent biological sample experiments were performed and examined by RNA-seq and protocols for data analysis as previously published (38–40). Therefore, a total of 12 individual samples were analyzed (Table 2). Alignments were established, and for each sample, a minimum of 1.4 to 4.4 million cDNA reads could be uniquely mapped to the NGR234 genome, resulting in 3 to 8 million uniquely mapped reads per treatment (Table 2). We verified that for the early-exponential-phase samples the fraction of mappable reads (on average, $\sim 38\%$) was 1.6-fold lower than that for the samples obtained in early stationary phase (up to 63%). Other researchers have already observed this variation in mappable reads depending on the selected culture conditions (44).

In the comparative analysis of RNA-seq data, we considered genes with a fold change of ≥ 2.0 and an adjusted *P* value of ≤ 0.05 as statistically significant and differentially expressed between two distinct conditions or states. Only values that complied with both requirements were used for subsequent analyses. Unless otherwise

specified, Tables 4 to 8 show only those transcriptomic data (data are mean values of two independent treatments) that revealed a fold change of ≥ 2.0 and an adjusted *P* value of ≤ 0.05 . The final set of differentially regulated genes is given in Table S1 in the supplemental material, and the highlights are discussed below.

A detailed evaluation of sense and antisense (AS) transcripts in all experiments revealed an AS transcript content ranging from 13 to 30%. These data suggest that a small but significant fraction of all genes in NGR234 is regulated through AS transcription. Earlier whole-transcriptome analyses have already emphasized the importance of AS and more recently the *cis*-AS regulation in prokaryotes (24, 45, 46).

TraI/R- and NgrI/R-specific gene regulation. It was determined that 316 genes (4.9% of all predicted genes) are regulated differently in the NGR234- $\Delta traI$ deletion mutant and the wild-type strain. Moreover, a total of 466 genes (7.3% of all predicted genes) were significantly altered in their expression profile in the NGR234- $\Delta ngrI$ deletion mutant (Fig. 2). Altogether, a common subset of 186 genes was differentially regulated in both mutant strains in comparison to the wild type (Fig. 2; see also Table S1 in the supplemental material). Surprisingly, almost 98% of these overlapping genes were identically up- or downregulated in the two strains. Thus, 130 genes appeared to be specifically expressed in the NGR234- $\Delta traI$ strain and 280 genes were uniquely regulated in the NGR234- $\Delta ngrI$ deletion mutant. All regulated genes were unequally distributed over the three NGR234 replicons (Table 4). The majority of all differentially regulated genes (65 to 70%) was observed on the bacterial chromosome (cNGR234), and only a very few genes were located on the symbiotic plasmid pNGR234a (Table 4). In the background of the NGR234- $\Delta traI$ strain, 13 pNGR234a-borne genes were significantly altered in their expression profile, and for the NGR234- $\Delta ngrI$ mutant, only eight differentially regulated genes were observed on this symbiotic replicon.

Expression analysis by qRT-PCR technology was used to partially confirm the RNA-seq data. Therefore, we analyzed the expression profiles of five different genes in the early stationary phase in the NGR234 wild type compared to both QS deletion mutants. We selected *rpoD* as the internal control gene and the following differentially regulated genes: *flgB* (NGR_c02740) (Table 5), *pilA* (NGR_c34640) (Table 5), NGR_b22870 (hypothetical protein possibly linked to T3SS-II) (Table 8), *exoI* (NGR_b18300) (Table 6), and NGR_c14830 (hypothetical protein; not listed in Tables 5 to 8). Expression data obtained for the five genes by qRT-PCR largely confirmed the data obtained by RNA-seq (see Table S2 in the supplemental material).

To date, only a few studies have performed genome-wide tran-

TABLE 5 T4P, flagellar biosynthesis, and chemotaxis-related genes significantly altered in their expression profile in both NGR234 QS deletion mutants^a

Gene no.	Locus tag	Predicted function	Fold change	
			$\Delta traI$	$\Delta ngrI$
1	NGR_c34710	Pilus assembly protein, TadB	+3.2	+3.3
2	NGR_c34700	Pilus protein ATPase, CpaF	+4.3	+3.5
3	NGR_c34690	Pilus assembly protein, CpaE	+4.5	+5.6
4	NGR_c34680	Pilus assembly protein, CpaD	+3.6	+3.7
5	NGR_c34670	Pilus assembly protein, CpaC	+3.3	+2.7
6	NGR_c34660	Pilus assembly protein, CpaB	+3.9	+4.1
7	NGR_c34640	Pilus assembly protein, PilA1	+11.0	+7.3
8	NGR_c34620	Pilus assembly protein, TadG	+5.0	+2.9
9	NGR_c34610	Pilus assembly protein, TadE	+4.6	+2.7
10	NGR_c03010	Flagellar biosynthesis protein, FlhA	+2.2	—
11	NGR_c02990	Flagellar basal body rod modification protein, FlgD	+10.9	+11.8
12	NGR_c02980	Flagellar biosynthesis repressor, FliB	+4.5	+3.9
13	NGR_c02970	Flagellar biosynthesis regulatory protein, FlaF	+11.3	+8.0
14	NGR_c02960	Flagellar hook-associated protein, FlgL	+22.9	+22.6
15	NGR_c02950	Flagellar hook-associated protein, FlgK	+15.2	+16.4
16	NGR_c02940	Flagellar hook protein, FlgE	+24.9	+23.3
17	NGR_c02930	Two-component transcriptional regulator	+10.5	+6.7
18	NGR_c02920	Lytic transglycosylase-like protein	+5.5	+5.1
19	NGR_c02910	Chemotaxis/motility protein, MotD	+8.9	+15.2
20	NGR_c02900	Chemotaxis/motility protein, MotC	+10.2	+10.8
21	NGR_c02890	Flagellar motor protein, MotB	+7.0	+8.4
22	NGR_c02880	Hypothetical protein	+8.2	+11.3
23	NGR_c02870	Flagellin protein, FlaD	+3.2	+4.7
24	NGR_c02850	Flagellin protein, FlaB	+2.4	—
25	NGR_c02810	Flagellar basal body L-ring protein, FlgH	+9.9	+10.9
26	NGR_c02800	Hypothetical protein	+24.9	+26.0
27	NGR_c02790	Flagellar basal body P-ring protein, FlgI	+25.3	+24.4
28	NGR_c02780	Flagellar P-ring biosynthesis protein, FlgA	+11.6	+12.3
29	NGR_c02770	Flagellar basal body rod protein, FlgG	+20.4	+20.3
30	NGR_c02760	Flagellar hook-basal body protein, FliE	+36.5	+27.2
31	NGR_c02750	Flagellar basal body rod protein, FlgC	+29.0	+25.9
32	NGR_c02740	Flagellar basal body rod protein, FlgB	+69.9	+82.2
33	NGR_c02720	Flagellum-specific ATP synthase, FilL	+12.2	+20.6
34	NGR_c02710	Flagellar basal body rod protein, FlgF	+14.0	(+11.6)
35	NGR_c02700	Hypothetical protein	+7.4	+8.1
36	NGR_c02690	Flagellar motor protein, MotA	+9.8	+8.8
37	NGR_c02680	Flagellar motor switch protein, FliM	+11.8	+11.6
38	NGR_c02670	Flagellar motor switch protein, FliN	+25.0	+28.6
39	NGR_c02660	Flagellar motor switch protein, FliG	+15.9	+14.0
40	NGR_c02630	LuxR family transcriptional regulator	+6.3	+5.5
41	NGR_c02620	LuxR family transcriptional regulator	+10.6	+6.5
42	NGR_c02610	Flagellar MS ring protein, FliF	+4.8	+4.9
43	NGR_c02600	Hypothetical protein	(+2.8)	+4.3
44	NGR_c02590	Chemoreceptor glutamine deamidase, CheD	+4.6	+6.7
45	NGR_c02580	Signal transduction response regulator	(+2.6)	+4.3
46	NGR_c02570	Chemotaxis-specific methyltransferase, CheB2	+4.0	+5.6
47	NGR_c02560	Chemotaxis protein methyltransferase, CheR	+4.7	+4.7
48	NGR_c02550	CheW family chemotaxis protein, CheW1	+2.8	+3.2
49	NGR_c02540	Chemotaxis protein, CheA2	+4.8	+6.6
50	NGR_c02530	Two-component response regulator receiver protein	+5.5	+5.3
51	NGR_c02520	Hypothetical protein	+6.9	+5.6
52	NGR_c02510	Chemotaxis methyl-accepting receptor protein	+4.2	+4.3
53	NGR_c00850	Methyl-accepting chemotaxis protein	+3.0	+4.2
54	NGR_c00530	Methyl-accepting chemotaxis protein	+3.9	+3.4
55	NGR_c20850	Methyl-accepting chemotaxis protein	+4.1	+4.2
56	NGR_b22620	Methyl-accepting chemotaxis protein	—	+3.2

^a Genes 1 to 9 code for the T4P, while genes 10 to 52 code for the flagellum or regulatory components and chemotaxis-associated genes identified within a large conserved cluster on cNGR234. Genes 53 to 56 are located elsewhere in the bacterial genome. $\Delta traI$, NGR234- $\Delta traI$ mutant strain; $\Delta ngrI$, NGR234- $\Delta ngrI$ mutant strain; —, transcriptome data did not match either of the two requirements (fold change of ≥ 2.0 ; adjusted P value of ≤ 0.05). Values in parentheses were specified for completeness and indicate an adjusted P value of 0.06 for NGR_c02710, 0.18 for NGR_c02600, and 0.09 for NGR_c02580.

TABLE 6 Exopolysaccharide biosynthesis genes differentially regulated in both NGR234 QS deletion mutants

Locus tag	Predicted function	Fold change ^b	
		$\Delta traI$	$\Delta ngrI$
NGR_b18410	Phosphomethylpyrimidine kinase, ThiD	-2.8	+2.9
NGR_b18400	Succinoglycan biosynthesis transporter, ExoP	-2.2	-3.6
NGR_b18390	UTP-glucose-1-phosphate uridylyltransferase	-2.8	-4.7
NGR_b18380	Succinoglycan biosynthesis protein, ExoO	-2.4	-4.6
NGR_b18370	Succinoglycan biosynthesis protein, ExoM	-2.6	-6.6
NGR_b18360	Succinoglycan biosynthesis protein, ExoA	-2.8	-5.5
NGR_b18350	Succinoglycan biosynthesis protein, ExoL	-2.6	-6.3
NGR_b18340	Endo-beta-glycanase, ExoK	-3.3	-5.7
NGR_b18330	Hypothetical protein	-4.1	-12.4
NGR_b18320 ^a	<i>rpoS</i> regulatory ncRNA (68 nt ^c), antisense	+36.0	+52.3
NGR_b18320 ^a	<i>rpoS</i> regulatory ncRNA (68 nt), sense	-2.4	-2.5
NGR_b18310	Hypothetical protein	-13.9	-15.9
NGR_b18300	Succinoglycan biosynthesis protein, ExoI	-29.5	-82.5
NGR_b18270	Exopolysaccharide production protein, ExoY	—	-3.1
NGR_b18260	Exopolysaccharide production protein, ExoF	—	-3.2
NGR_b18250	Succinoglycan biosynthesis protein, ExoQ	—	-3.4
NGR_b18240	Exopolysaccharide production protein, ExoZ	—	-2.5
NGR_b18220	ABC transporter ATP-binding protein, ExsA	-2.0	-2.1
NGR_b18180	Succinoglycan biosynthesis regulator, ExsB	—	-3.0
NGR_b18140	ExsI protein	—	-3.8
NGR_b15690	Endo-beta-glycanase, ExsH	-13.6	-20.1
NGR_a00830	Exopolysaccharide repressor protein	-3.1	-5.0

^a Data for NGR_b18320 showed it to be significantly differentially regulated at the sense and antisense transcription level.

^b $\Delta traI$, NGR234- $\Delta traI$ mutant strain; $\Delta ngrI$, NGR234- $\Delta ngrI$ mutant strain; —, transcriptome data did not match either of the two requirements (fold change of ≥ 2.0 ; adjusted *P* value of ≤ 0.05).

^c nt, nucleotides.

scriptome analyses to identify QS-regulated gene expression patterns in response to exogenous AHLs in bacteria. One of the best-studied model organisms in this research field with respect to QS is the opportunistic pathogenic bacterium *P. aeruginosa*. Several studies have been published analyzing the *P. aeruginosa* QS-dependent transcriptome using microarray technologies and RNA sequencing (27, 44, 47–50). Since the overall setups of these studies were slightly different, the number of genes that were differentially regulated in response to QS processes varied. While in the study by Wagner et al. (47) 11.1% of all genes appeared to be QS dependent, in the study by Schuster et al. (48) 6.3% and in the study by Hentzer and colleagues (49) only 2.9% of all genes were

identified that appeared to be differentially regulated through AHLs. Only very recently, Chugani et al. reported on strain-dependent diversity of *Pseudomonas* QS-dependent gene expression. They observed that the QS regulons represent ~0.5 to 6.2% of the coding sequences for a given *P. aeruginosa* genome (27). Similarly, for the Gram-negative pathogenic bacterium *Yersinia pestis*, a total of 335 genes were reported to be QS dependently regulated (51). This equals 8% of the *Y. pestis* genome, which is 4.83 Mbp in size and contains 4,221 open reading frames (ORFs) (52). With respect to these studies, a total of 4.9% differentially regulated genes in the NGR234- $\Delta traI$ background and a total of 7.3% in NGR234- $\Delta ngrI$ seem to be reasonable. The overall number of QS-regulated genes in NGR234 appears to be slightly higher than those numbers published for the closely related *S. meliloti*. In this organism, a minimum of 55 to 170 genes were linked to a QS-dependent regulatory circuit (16, 19, 20).

Function-based interpretation of transcriptome data. The differentially expressed genes in both mutants and the parent strain were classified into seven functional categories based on the KEGG database (<http://www.genome.jp/kegg/pathway.html>). As indicated in Fig. 3A and B, the genome-wide transcriptome data analysis revealed that upregulated genes were mainly linked to motility, regulators, general metabolism, cell wall and succinoglycan biosynthesis (cell envelope), transporters (mostly ABC), and quite a significant number of hypothetical proteins. Striking changes in gene expression of the most important functional categories are discussed below.

Two hypothetical proteins show the highest expression level in both mutants. Within the set of differentially regulated genes detected in both mutants, a relatively high number of 94 genes in

TABLE 7 Upregulated cofactor biosynthesis genes in NGR234- $\Delta ngrI$

Locus tag	Predicted function	Fold change
NGR_c25140	Biotin synthase, BioB	+3.0
NGR_c25130	8-Amino-7-oxononanoate synthase, BioF	+3.5
NGR_c25120	Dethiobiotin synthetase, BioD	+3.3
NGR_c25110	Adenosylmethionine-8-amino-7-oxononanoate aminotransferase, BioA	+2.8
NGR_c25100	Biotin synthesis protein, BioZ	+4.7
NGR_c13770	Biotin transport regulator, BioS	+6.3
NGR_b03300	Coenzyme PQQ synthesis protein, PqqE	+7.8
NGR_b03290	Coenzyme PQQ synthesis protein, PqqD	+9.7
NGR_b03280	Coenzyme PQQ synthesis protein, PqqC	+10.0
NGR_b03270	Coenzyme PQQ synthesis protein, PqqB	+10.7
NGR_b03260	Coenzyme PQQ synthesis protein, PqqA	+9.9
NGR_b03250	Alcohol dehydrogenase	+9.5
NGR_b03240	LuxR family transcriptional regulator	+3.0

TABLE 8 T3SS-II-related genes and their fold changes in NGR234- $\Delta traI$ and NGR234- $\Delta ngrI$

Locus tag	Predicted function	Fold change ^b	
		$\Delta traI$	$\Delta ngrI$
NGR_b23040 ^a	Hypothetical protein	—	-3.8
NGR_b23030 ^a	Hypothetical protein	—	-2.8
NGR_b23010	Hypothetical protein possibly linked to T3SS-II	—	—
NGR_b23000	Type III secretion component, RhcT	—	-3.3
NGR_b22990	Type III secretion component, RhcS	—	-4.9
NGR_b22980	Translocation protein, RhcR	—	-5.5
NGR_b22970	Translocation protein, RhcQ	—	-5.1
NGR_b22960	Type III secretion component, RhcZ	—	-6.7
NGR_b22950	Type III secretion component, RhcN	—	-5.2
NGR_b22940	Type III secretion component, YOP protein/translocation protein L	—	-4.2
NGR_b22930	Putative type III secretion component	—	-4.6
NGR_b22920	Type III secretion component, RhcJ	-2.1	-4.0
NGR_b22910	Hypothetical protein possibly linked to T3SS-II	—	-4.8
NGR_b22900	Hypothetical protein possibly linked to T3SS-II	—	-4.6
NGR_b22890	Type III secretion component, RhcCl	—	-3.9
NGR_b22880	Hypothetical protein possibly linked to T3SS-II	-2.9	-3.9
NGR_b22870	Hypothetical protein possibly linked to T3SS-II	-3.7	-4.1
NGR_b22860	Hypothetical protein possibly linked to T3SS-II	-3.3	-4.4
NGR_b22850	Hypothetical protein possibly linked to T3SS-II	-3.3	-5.6
NGR_b22840	Type III secretion component, RhcV	-2.6	-4.5
NGR_b22830	Type III secretion component, RhcC2	-2.7	-5.4
NGR_b22820	Hypothetical protein possibly linked to T3SS-II	-2.3	-3.2
NGR_b22810	Hypothetical protein possibly linked to T3SS-II	-2.6	(-3.3)
NGR_b22800	Translocation protein, RhcU	-2.3	-4.3
NGR_b22790 ^a	Protein precursor, ErfK/SrfK	—	-3.7

^a Genes were not directly linked to the T3SS-II cluster but were located upstream/downstream and were obviously simultaneously regulated.

^b $\Delta traI$, NGR234- $\Delta traI$ mutant strain; $\Delta ngrI$, NGR234- $\Delta ngrI$ mutant strain; —, transcriptome data did not match either of the two requirements (fold change, ≥ 2.0 ; adjusted *P* value, ≤ 0.05). Value in parentheses, adjusted *P* value of 0.08.

NGR234- $\Delta ngrI$ and 62 genes in the NGR234- $\Delta traI$ background were classified as hypothetical proteins. It is noteworthy that among these, the two most strongly regulated genes were identified. These were the ORFs NGR_c14820 and NGR_c14830. Both are located on cNGR234 flanking each other but are transcribed in opposite directions. In the NGR234- $\Delta traI$ mutant strain, NGR_c14820 was 32-fold downregulated by antisense transcripts and NGR_c14830 was 41-fold downregulated by sense transcripts. Further, an even stronger regulation was observed for both genes in the NGR234- $\Delta ngrI$ background, where NGR_c14820 was 46-

fold (antisense) and NGR_c14830 was up to 132-fold (sense) downregulated. Interestingly, no clear function could be assigned to these genes.

Genes linked to general cell and energy metabolism and transport. Previous studies have reported that QS can have profound effects on growth, nodulation efficiency, and nodule development in various rhizobial species (14–16, 19, 20, 53–55). Within this framework, we found that several genes which are related to either energy production, sugar uptake, or respiration were significantly altered in their gene expression levels in either NGR234- $\Delta traI$, NGR234- $\Delta ngrI$, or both mutants (Fig. 3A and B). Among genes that potentially influence growth were several that encode ATP synthase subunits (NGR_c04460 to -c04500 and NGR_c31110 to -c31140), which were 2- to 4.6-fold downregulated in the background of NGR234- $\Delta ngrI$.

In addition, NGR234 contains four loci encoding cytochrome *c* and Cbb3-type cytochrome *c* oxidases, all located on cNGR234. While one of these clusters (NGR_c25510 to -c25550) appeared to be not differentially expressed, almost all genes located in the cluster stretching from NGR_c05230 to NGR_c05300 showed a 2- to 4-fold-reduced expression level in the NGR234- $\Delta traI$ mutant. In the background of NGR234- $\Delta ngrI$, only two out of the six cytochrome *c* oxidase genes were significantly downregulated. The cluster ranging from NGR_c25780 to NGR_c25810 was only partially downregulated in the NGR234- $\Delta traI$ mutant. A detailed analysis of regulated genes within our transcriptomic data revealed that the Cbb3-type cytochrome *c* oxidase cluster stretching from NGR_c17970 to NGR_c17990 was regulated (fold change,

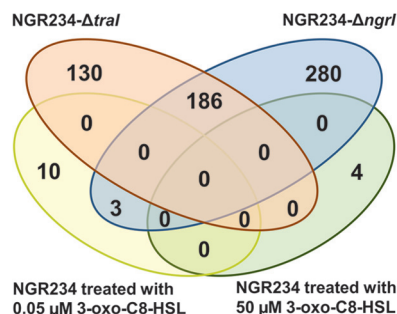


FIG 2 Venn diagram showing the overlap of differentially expressed genes (fold change, ≥ 2.0 ; adjusted *P* value, ≤ 0.05) among NGR234 AI synthase mutants and AHL treatments. The ellipses display the number of uniquely regulated genes in each NGR234 mutant versus the parental strain and for each AHL treatment versus the parental strain. The ellipses also show the number of commonly regulated genes within particular relationships. Only the NGR234 AI synthase mutants share a core set of 186 differentially regulated genes.

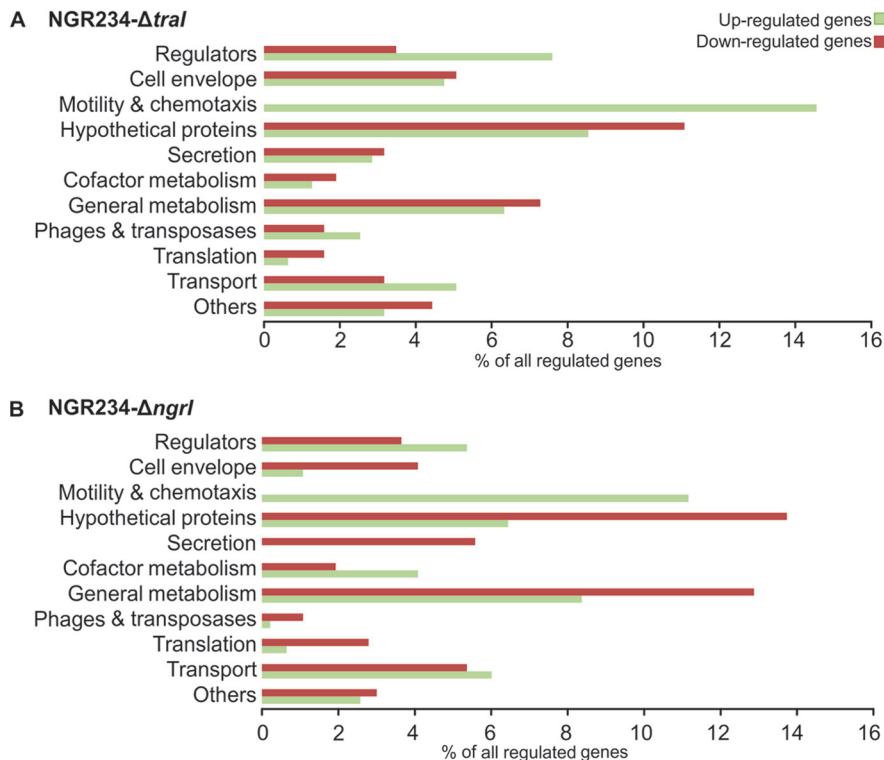


FIG 3 Differentially expressed genes (%) in NGR234 mutant strains. (A) In the background of NGR234- Δ traI versus the parent strain. (B) In the background of NGR234- Δ ngrI versus the parent strain. The classification was based on the KEGG database (<http://www.genome.jp/kegg/pathway.html>).

≥ 2.0 ; P value of ≤ 0.3 ; data not shown) in NGR234- Δ traI and NGR234- Δ ngrI. Although this cluster did not meet our requirements for significantly, differentially regulated genes, data in Fig. 4A clearly indicate a regulation of the Cbb3-type cytochrome *c* oxidase genes. Interestingly, genes within this cluster were up-regulated in NGR234- Δ traI and downregulated in NGR234- Δ ngrI.

In this context, we also found genes linked to nitric oxidase reduction and stress response, which were differentially expressed in the mutant strains (fold change, ≥ 2.0 ; P value of ≤ 0.5 ; data not shown) (Fig. 4A). Similar to the above-mentioned regulation of the *cbb3*-type cluster, the nitric oxidase genes were upregulated in NGR234- Δ traI and downregulated in NGR234- Δ ngrI.

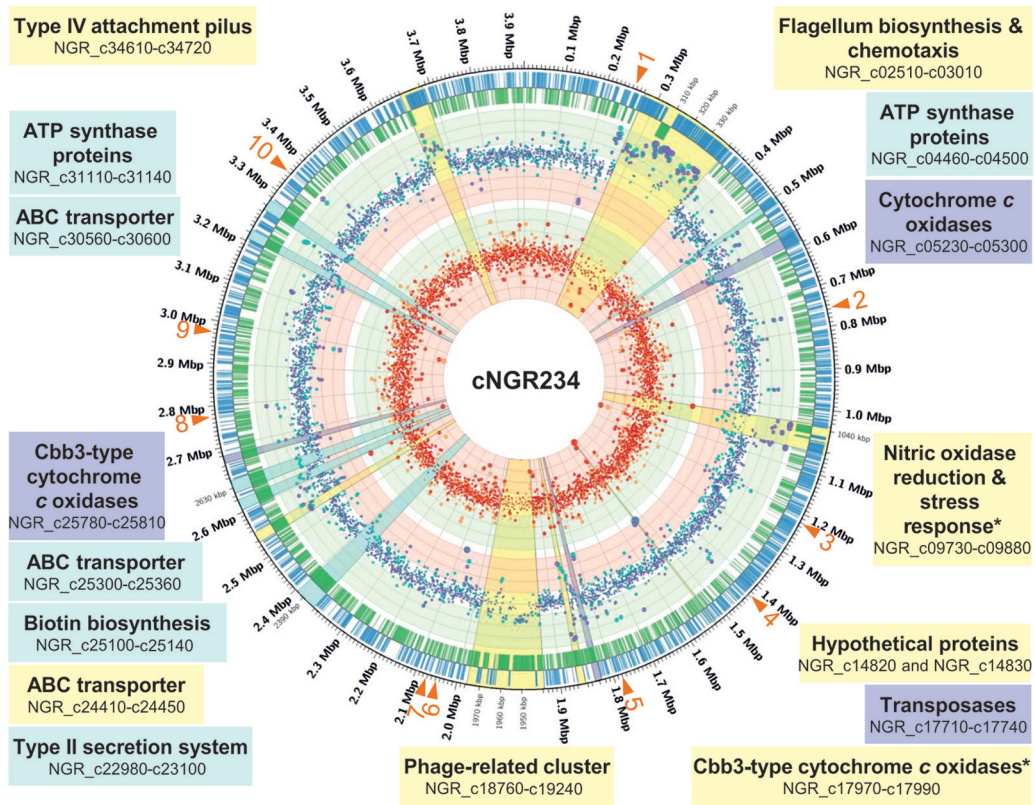
Further, several of the ribosomal subunits (*rplJ*, *rpmH*, *rpmG*, *rpmB*, *rpmJ*, and *rpsT*) were significantly reduced in their expression in both mutants. While *rplJ* was downregulated in NGR234- Δ traI, the ribosomal subunits *rpmH*, *rpmG*, *rpmB*, *rpmJ*, and *rpsT* were all downregulated in the NGR234- Δ ngrI mutant. Furthermore, several tRNA synthase and tRNA genes were downregulated in both mutants, and in addition, a few ABC-type transporters for different sugars were also subject to a QS-dependent regulation. Finally, more than 30 regulators and two regulatory noncoding RNAs (ncRNAs) (NGR_b18320 and NGR_b21180) out of five were subject to a QS-dependent regulation in the two mutant strains (Fig. 3A and B; see also Table S1 in the supplemental material).

Motility and chemotaxis genes are upregulated in NGR234- Δ traI and NGR234- Δ ngrI. Among the genes that were most strongly upregulated in both mutant strains, over 50 genes were involved in flagellum biosynthesis, pilus attachment, and che-

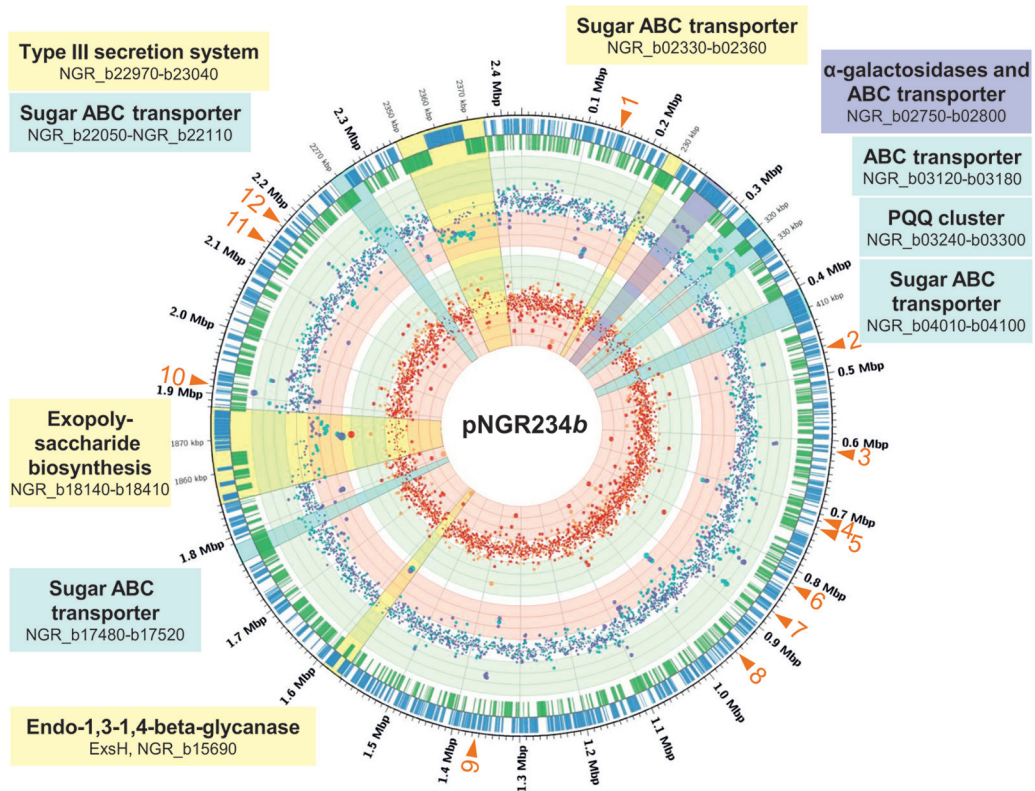
motaxis (Table 5; Fig. 4A; see also Fig. S3A and B in the supplemental material). The NGR234 chromosome encodes a single flagellum, which is involved in bacterial motility and chemotaxis. The flagellar genes are mainly organized in a single large cluster encompassing more than 40 genes and spanning from NGR_c02610 to NGR_c03010 (Table 5). Most of the flagellum-specific genes were more than 10-fold and some even up to 80-fold up-regulated in their transcription in NGR234- Δ traI and NGR234- Δ ngrI compared to the parent strain (Table 5). Therefore, *flgB* expression was verified by qRT-PCR (see Table S2). Moreover, these findings are consistent with the above-observed motility phenotypes in sedimentation assays where both mutants were not able to settle within the given time period (Fig. 1). Our data are in agreement with earlier findings reported for planktonic *Bradyrhizobium japonicum* cells and for *S. meliloti* suggesting that flagella play a pivotal role during root colonization but that they are most likely not essential during the infection process (56–59). This hypothesis fits well with the recent observation that flagellar genes are downregulated in bacteroids in NGR234 (29) and with the observation that flagellar genes are subject to QS-mediated regulation in *S. meliloti* (60, 61).

Further, the NGR234 genome contains several gene clusters involved in the biosynthesis of type IV attachment pili (T4P). T4P are involved in motility, attachment to surfaces, biofilm formation, twitching motility, and virulence (62), and they are of importance for an initial attachment to the root surface (63). We have previously identified two clusters of T4P-encoding genes on pNGR234b along with a third cluster of 12 genes on the chromosome (NGR_c34610 to -c34720) (13). While the two clusters on pNGR234b were not affected in their transcription levels, the

A



B



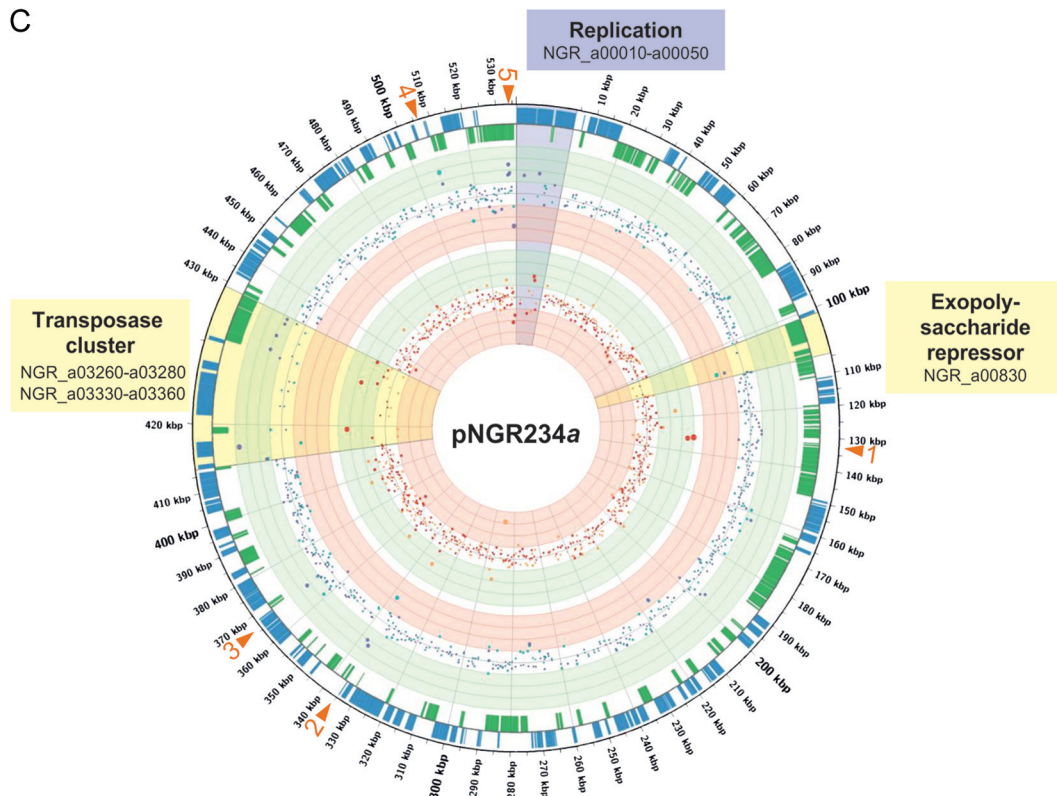


FIG 4 Circular representation of the complete RNA-seq-based transcriptome data set of NGR234- $\Delta traI$ and NGR234- $\Delta ngrI$ versus the parent strain for all three replicons (A to C) generated with the Circos 0.64 software (99). The following specifications apply for panels A to C. Fold change cutoff is $\log_2 4/-4$ (circle size by values). Circles are described from the outside to the innermost circle: the outer circles indicate the coordinates of cNGR234, pNGR234b, and pNGR234a in megabase pairs and positions of several regulated regions/genes that are not explicitly mentioned in the text. The positions are tagged with orange arrows and corresponding numbers. These genes/ORFs are listed in detail for panels A, B, and C, respectively. Note that several genes within the marked regions have adjusted P values of ≥ 0.05 . The second and third outer circles indicate ORFs on the leading (blue) and the lagging (dark green) strands. The next circles are light green areas that indicate $\log_2 4, 3, 2,$ and 1 (from outside to inside); the next circles, represented by purple and cyan dots (scattered over light green/white/light red areas), are sense transcripts for NGR234- $\Delta traI$ (purple) and NGR234- $\Delta ngrI$ (cyan); the light red circles/areas are $\log_2 -1, -2, -3,$ and -4 (from outside to inside). The next light green and light red areas apply as described above. The following inner circles represented by red and orange dots (scattered over light green/white/light red areas) are antisense transcripts for NGR234- $\Delta traI$ (red) and NGR234- $\Delta ngrI$ (orange). Highlighted areas are 5-fold magnified and show regions/genes which are differentially regulated in the mutant strains and are further discussed in the text. Light yellow areas, regions/genes regulated in both mutants (NGR234- $\Delta traI$ and NGR234- $\Delta ngrI$); light purple areas, regions/genes regulated only in NGR234- $\Delta traI$; light cyan, regions/genes regulated only in NGR234- $\Delta ngrI$. (A) Circular representation of RNA-seq data for cNGR234. Highlighted areas marked with asterisks include also adjusted P values of ≥ 0.05 . Tagged positions: 1, hypothetical proteins with ice nucleation domain (NGR_c02320 to -c02360); 2, phosphosulfate reductase/sulfate adenylyltransferases (NGR_c06940 to -c06960); 3, hypothetical proteins (NGR_c11390 to -c11590); 4, nitrogen fixation proteins (NGR_c17900 to -c17930); 5, hypothetical proteins and transposases (NGR_c13830 to -c13890); 6, MerR family transcriptional regulator (NGR_c19960); 7, calcium binding hemolysin-like protein (NGR_c20180); 8, acetyl coenzyme A (acetyl-CoA) synthetase (NGR_c26750); 9, hypothetical protein (NGR_c28550); 10, hypothetical protein (NGR_c31960). (B) Circular representation of RNA-seq data for pNGR234b. For specifications of individual circles, see above. Tagged positions: 1, putative secretion protein and putative nuclease inhibitor (NGR_b01620 to -b01640); 2, hypothetical protein (NGR_b04610); 3, hypothetical proteins (NGR_b06210 and NGR_b06130); 4, alanine racemase and D-amino acid dehydrogenase (NGR_b07050 to -b07070); 5, copper-related proteins (NGR_b07130 to -b07180); 6, copper-related proteins (NGR_b08240 to -b08280); 7, C₄-dicarboxylate transport system (NGR_b08880 and NGR_b08920); 8, hypothetical proteins (NGR_b09530 and NGR_b09550); 9, hypothetical proteins (NGR_b13550 and NGR_b13560); 10, hypothetical protein (NGR_b18740); 11, propionyl-CoA carboxylases (NGR_b20820 to -b20920); 12, adenylate cyclase (NGR_b21170). (C) Circular representation of RNA-seq data for pNGR234a. For specifications of individual circles, see above. Tagged positions: 1, ferredoxin and hypothetical protein (NGR_a01050 and NGR_a01060); 2, precursor of 26.2 kDa for periplasmic protein and outer membrane protein (NGR_a02560 and NGR_c02570); 3, hypothetical proteins (NGR_a02770 to -a02800); 4, hypothetical protein (NGR_a03910); 5, conjugal transfer cluster (NGR_a03950 to -a04210).

chromosome-carried T4P genes were nearly all 3- to 11-fold up-regulated (Table 5). The overall changes in T4P transcription in the NGR234- $\Delta ngrI$ and the NGR234- $\Delta traI$ mutant were quite similar (Table 5; Fig. 4A), and for *pilA*, they were verified by qRT-PCR in both mutants (see Table S2 in the supplemental material). This observation is in line with reports on an altered surface motility of a *sinI* mutant in *S. meliloti* (19) and correlates well with observations made for QS-dependent expression of T4P and surface motility in *P. aeruginosa* (64).

Succinoglycan biosynthesis is repressed in NGR234- $\Delta traI$ and NGR234- $\Delta ngrI$. The development of the *Rhizobium*-legume symbiosis requires the timely and spatially regulated bacterial synthesis of four classes of cell envelope-associated polysaccharides: the cyclic β -(1,2)-glucans, the outer membrane lipopolysaccharides (LPSs), the external capsular polysaccharides (KPS), and finally the extracellular polysaccharides (exopolysaccharides [EPSs]) composed of succinoglycan [EPS I] and galactoglucan [EPS II] (65). NGR234 carries several clusters and operons involved in the

synthesis of the bacterial exopolysaccharides, capsular polysaccharides, and lipopolysaccharides (13, 66). The largest of these clusters (encompassing *exo* and *exs* genes) stretches from *thiD* to *exsI* with a total of 31 genes encoding the synthesis of low-molecular-weight exopolysaccharides (67, 68). This large cluster is located on pNGR234*b*, and its overall genetic organization is highly similar to that of the corresponding *exo/exs* cluster on the pSymB replicon of *S. meliloti* (67, 69). The most striking differences are mainly found in proximity to the *exoI* gene (NGR_b18300).

Our analysis suggests that most of the genes within the conserved *exo* cluster are downregulated in both the NGR234- Δ *traI* and the NGR234- Δ *ngrI* mutant strains compared to the parent strain (Fig. 4B). The *exoI* gene and a flanking hypothetical protein (NGR_b18310) were strongly repressed in their expression in both mutants on the level of sense transcription (see Fig. S3C in the supplemental material). While *exoI* was 83-fold and NGR_b18310 was 16-fold downregulated in NGR234- Δ *ngrI* (Table 6), the remaining significantly regulated genes within this cluster were not as strongly affected in their expression level.

Within the conserved *exo* cluster, a small 68-nucleotide non-coding RNA was observed that was strongly upregulated on the level of antisense transcription. While the respective ncRNA gene was weakly repressed by sense transcription, by a factor of only 2.4 and 2.5 in both mutant strains, the antisense *rpoS*-like ncRNA of NGR_b18320 was 52-fold upregulated in NGR234- Δ *ngrI* and 36-fold upregulated in NGR234- Δ *traI* (Table 6). Although we do not know the exact target of this ncRNA, it is likely that it interacts with EPS biosynthesis and further suppresses the transcription of the indicated *exo* cluster in the absence of AI molecules. BLAST analyses accomplished with NGR_b18320 revealed that this ncRNA was present only in the genomes of the broad-host-range strains *S. fredii* USDA257 and HH103 but not in *S. meliloti* 1021. We have previously identified the flanking regions of this ncRNA on pNGR234*b* next to *exoI* as part of a region in which gene rearrangement and deletions in the EPS cluster, compared to *S. meliloti* 1021, had been observed (67).

With respect to biosynthesis and regulation of EPS, *S. meliloti* appears to be one of the best-studied model organisms (65). In this strain, the ExpR/Sin QS system controls the expression of the succinoglucan biosynthesis genes (16, 70). Here, the observation that the EPS biosynthesis is also subject to a QS-dependent regulation in NGR234 fits well with the previous observations for *S. meliloti* (65 and references therein). However, in *S. meliloti* 1021 only a single AI synthase has been identified, while NGR234 encodes two AI synthases.

Cofactor biosynthesis genes are upregulated in NGR234- Δ *ngrI*. Beside its role as a cofactor in carboxylation reactions, biotin plays a pivotal role during root colonization in sinorhizobia (71). It is of importance for the synthesis and degradation of polyhydroxybutyrate (72) and various anaplerotic reactions in rhizobia and bradyrhizobia (73, 74). A minimum set of six genes is generally required for biotin biosynthesis in Gram-negative bacteria, and they are usually organized within a single transcriptional unit (75). In NGR234, five essential biotin synthesis genes, *bioADBZ* (NGR_c25100 to -c25140), are clustered on the chromosome, whereby a *bioA* (NGR_b06270) homolog and a *bioF* (NGR_b10670) ortholog can also be found on pNGR234*b*. In addition, the regulatory locus *bioS* (NGR_c13770) was identified on the chromosome. Furthermore, this gene was detected only in species closely related to *Sinorhizobium fredii*. A copy of the sixth

biotin synthesis gene, *bioC* (NGR_c26660), is located further downstream of the *bioADBZ* cluster. Genes involved in biotin transport (*bioMNY*) were identified elsewhere on the chromosome.

The transcriptomic data set showed that the genes *bioADBZ* together with the *bioS* regulator were upregulated in the NGR234- Δ *ngrI* mutant. The biotin biosynthesis genes were on average 3-fold upregulated, while the *bioS* gene was almost 6.5-fold upregulated by sense transcripts (Table 7). Since it can be assumed that TY medium contains high levels of this vitamin, the induced regulation of the biotin biosynthesis genes in the absence of the *ngrI*-specific AI suggests a QS-dependent regulation of this *bio* cluster. With respect to the regulation of biotin, this is the first report showing a QS-dependent regulation of bacterial biotin biosynthesis genes.

The *bioS* gene is unique to the sinorhizobia, and it is involved in regulation of biotin-dependent processes and survival under biotin starvation in *S. meliloti* (76, 77). Interestingly, earlier we reported on a possible link between the *bioS* regulation and QS-dependent gene regulation in *S. meliloti* (75). This observation is now supported by the transcriptome data in the background of the NGR234- Δ *ngrI* strain (Table 7; Fig. 3B).

Pyroloquinoline quinone (PQQ) is required as a cofactor for dehydrogenases involved in the primary oxidation of growth substrates such as alcohols (ethanol, glycerol, and polyvinyl alcohols), amines, and aldose sugars. PQQ-dependent dehydrogenases are mostly secreted into the bacterial periplasm (78). While the presence and function of PQQ enzymes have been reported in many rhizobial genomes, only little is known about their role during root infection and nodule formation. In this respect, the presence of a PQQ-dependent glucose dehydrogenase appears to be essential for nodulation efficiency and competitiveness in *S. meliloti* (79, 80).

In the NGR234 genome, five genes encode the PQQ biosynthesis. The *pqqEDCBA* genes are located on pNGR234*b* in a single cluster (NGR_b03260 to -b03300) together with a possible alcohol dehydrogenase (NGR_b03250) and a potential LuxR regulator (NGR_b03240) (Table 7). In our study, all genes within the PQQ gene cluster were strongly upregulated (up to 10.7-fold) in the NGR234- Δ *ngrI* mutant but not in the NGR234- Δ *traI* mutant (Fig. 4B). This finding suggests that PQQ-associated genes are regulated and controlled by NGR234 QS signaling that is *ngrI* specific. This is a novel finding, since it has previously not been reported that PQQ genes in NGR234 are subject to QS-dependent regulation.

T2SS and T3SS-II are subject to QS-dependent regulation. NGR234 carries a remarkable number of secretion-associated genes (13). Within this framework, we asked the question to what extent the many secretory genes are subject to a QS-dependent gene regulation in NGR234.

Expression of several T2SS-associated genes is diminished. The general secretion-related pathway (T2SS) is widely conserved in Gram-negative bacteria and translocates exoproteins (e.g., cellulases, lipases, etc.) from the bacterial periplasm into the surrounding medium. The T2SS is formed by a set of 12 to 16 proteins (GspA to GspS), and in many ways they resemble type IV pilus assembly systems (81). In NGR234, these genes are required for type II pilus assembly and are all located in a single cluster on cNGR234 encompassing 13 genes (NGR_c22980 to -c23100). With respect to the regulation of secretion pathways, it is notable

that several of the general secretion pathway-related genes were significantly downregulated in the NGR234- $\Delta ngrI$ mutant (Fig. 4A).

QS-mediated repression of the T3SS-II. Among the many secretion systems that are encoded on the genome of NGR234, we reported on two clusters of genes involved in the buildup of two distinct type III secretion apparatuses (T3SS). Many Gram-negative bacteria utilize T3SS to direct effector proteins into the cytoplasm of their eukaryotic hosts. These specialized protein export machineries are important components of bacterial virulence (82). In NGR234, the first T3SS (T3SS-I) is encoded on the symbiotic plasmid (pNGR234a) and a second T3SS (T3SS-II) was identified on pNGR234b. The two loci each encompass 22 genes involved in the assembly of the two secretion machineries (13, 83). The T3SS-I locus was found to be one of the key determinants of host range (84–86). Recently, it was also shown that the T3SS-I locus was upregulated in the *Leucaena leucocephala* and *V. unguiculata* bacteroids. Transcription was, however, highest in the *L. leucocephala* nodules in comparison to the *V. unguiculata* nodules (29). Within this framework, our transcriptome study suggests that the T3SS-I is subject to a QS-independent regulation. This observation fits well with the reports on the flavonoid- and NodD1-SyrM1-NodD2-TtsI-dependent regulatory cascade controlling the activity of the T3SS-I locus (86, 87). In contrast to the T3SS-I, not much is known about the function of the second T3SS locus. Only a few of the T3SS-II-associated genes were upregulated in *L. leucocephala* bacteroids (29), and a deletion of NGR_b22890 to NGR_b22950 in the T3SS-II did not result in a symbiotic phenotype, suggesting that the T3SS-II locus is not required for effective nodulation of the few legumes tested (13, 88). In contrast to the QS-independent regulation of T3SS-I, the T3SS-II, however, appears to be regulated in a QS-dependent manner. Our transcriptome analysis of the NGR234- $\Delta ngrI$ mutant suggests that all genes within the T3SS-II locus (NGR_b22790 to -b23040) were downregulated by a factor of 3 to 7 compared to the parent strain (Table 8; see also Fig. S3D in the supplemental material), and for NGR_b22870, qRT-PCR analyses verified these findings (see Table S2). Interestingly, in the NGR234- $\Delta tral$ strain only 10 genes (NGR_b22920 and NGR_b22880 to -b22800) were regulated in a QS-dependent manner, suggesting a slightly different expression with respect to the *tral*-dependent regulation.

QS-dependent regulation of transposase activities in NGR234. The NGR234 genome encodes a significant number (4.1%) of phages and transposases which are unequally distributed over the three replicons (13). On pNGR234a, 114 transposases and, on pNGR234b, 142 transposases were observed, whereas only 79 transposable elements were found on the chromosome. Insertion sequence (IS) elements could be grouped into 36 families, the largest of which includes 10 copies of the NGRIS-4 transposable element, and their sizes range from 623 to 3,316 bp. With respect to our transcriptome study, it was obvious that altogether 14 transposases were regulated in a QS-dependent manner in the NGR234- $\Delta tral$ mutant. In the NGR234- $\Delta ngrI$ mutant, five transposases were significantly repressed in their expression levels, while only one was induced.

In NGR234, several phage-related proteins have been identified during the genome analysis. Most strikingly, a large cluster comprising 49 phage-related genes was carried on the bacterial chromosome (Fig. 4A). In the background of the NGR234- $\Delta ngrI$

mutant, several genes within this cluster were 3- to 4-fold down-regulated.

Nodulation is not affected in *tral* or *ngrI* deletion mutant strains. Our transcriptome data revealed that almost none of the symbiotic loci were differentially regulated in the NGR234 mutants (Fig. 4C). To further verify these findings, we performed nodulation assays to monitor the nodulation phenotype of the different AI synthase mutants versus the parent strain. The assays revealed that the QS deletion mutants were able to form nitrogen-fixing nodules on *V. unguiculata*, *V. radiata*, and *T. vogelii* and did not differ significantly in their nodulation efficiencies from the NGR234 wild type (see Table S3 in the supplemental material). We further tested the nodulation phenotype of the NGR234 double mutant with a deletion in both QS loci. Similarly, the NGR234- $\Delta ngrI/\Delta tral$ mutant was not affected in its ability to form nitrogen-fixing nodules. Altogether, these observations fit well with the hypothesis that QS is perhaps not of crucial importance for nodulation *per se*.

AHL-dependent gene expression in early exponential phase of NGR234. NGR234 carries a remarkably high number of genes, which are involved in the degradation of various AHL signaling molecules (55). It is worthwhile to speculate whether NGR234 uses this quorum quenching (QQ) arsenal to regulate its own AI concentration inside and outside the cell or whether the QQ-based strategy provides NGR234 a competitive advantage in the rhizosphere. The intertwined regulation of these QQ-associated genes is still unsolved and so far could not be linked to the presence of various levels of AHLs. In our experimental setup, we wanted to investigate the influence of different AHL concentrations on the expression of NGR234's QQ loci. Therefore, we used RNA-seq to analyze overall changes in the expression profiles of NGR234 cells challenged with externally added AHLs.

In order to answer the question whether the QQ-related genes could be induced by the addition of AHLs, we treated exponentially growing cells with 3-oxo-C₈-HSL at two different concentrations (0.05 μ M and 50 μ M). Interestingly, none of the previously identified QQ genes showed an increased transcription level due to the added AHLs. To our surprise, we identified only a few genes that were significantly altered in their transcription profile (Fig. 2; Table 4) under both conditions. The addition of 0.05 μ M 3-oxo-C₈-HSL identified 13 significantly regulated genes, and the addition of 50 μ M merely identified four significantly differently regulated genes compared to equally treated NGR234 wild-type cells.

The observation that only a few genes were significantly altered in their expression profiles suggests that QS-dependent gene regulation is less important during exponential growth in NGR234 and that factors other than just an increase in external AHL levels are required for a QS-dependent gene expression. It is noteworthy that other studies have already reported on QS modulators like QscR and antiactivators like QsIA that regulate the timing of QS-controlled gene expression and the threshold concentration of the QS signal (89, 90).

Rhizopine catabolism is repressed in the presence of high levels of AHLs. Surprisingly, in the presence of high concentrations of AHLs (50 μ M) all four differentially regulated genes could be grouped to the cluster responsible for rhizopine catabolism collectively called the *moc* operon. Rhizopines are secreted plant compounds, which are synthesized by bacteroids inside the plant nodule in *Rhizobium*-legume interactions. Plant-nodulating rhi-

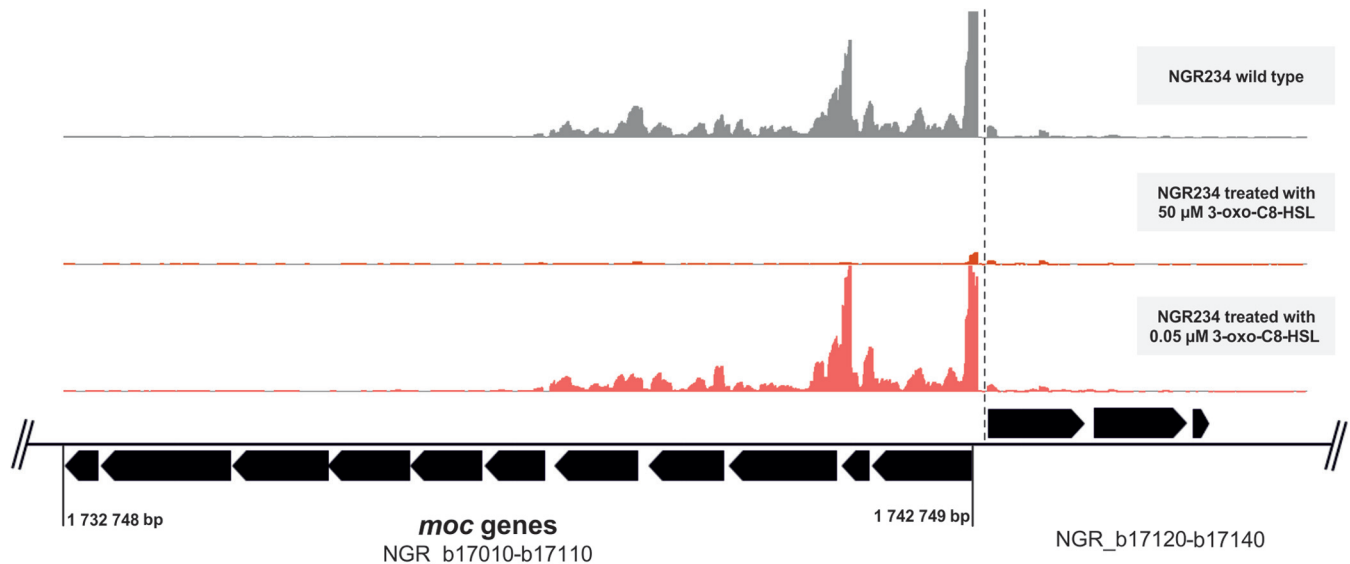


FIG 5 Partial physical map of rhizopine catabolism genes (*moc* genes) located on pNGR234b (NGR_b17010 to -b17110) and the relevant transcriptome profiles for NGR234 wild type (control), NGR234 treated with high levels of AHLs (50 μ M 3-oxo-C₈-HSL), and NGR234 treated with moderate levels of AHLs (0.05 μ M 3-oxo-C₈-HSL). Transcriptome profile images of the leading and lagging strand were generated with IGB (40), merged (indicated with a dashed line), and visualized on the leading strand for a simplified presentation. The *y* axis scale cutoff was set to 800 (leading strand) and to -800 (lagging strand). Black arrows indicate the ORFs identified within and flanking the *moc* region of NGR234.

zobia like NGR234 can obtain a nutritional advantage and a competition success for nodule formation from these symbiotic associations as the plant-associated rhizopines stimulate rhizobial growth (91–93). These compounds function as growth substrates and are catabolized by free-living rhizobia located in nodule infection threads and in the rhizosphere (94). In NGR234, the *moc* gene cluster, which is involved in the degradation of rhizopines, is composed of six genes of which four, *mocABRC*, are essential for the catabolic function. The NGR234 *moc* cluster is located on pNGR234b, probably stretching from NGR_b17010 to NGR_b17110. In our transcriptome data, *moc* genes ranging from NGR_b17080 to -b17110 (Fig. 5) were 9- to 12-fold downregulated in NGR234 challenged with 50 μ M 3-oxo-C₈-HSL. The *moc* genes have been previously observed to be subject to QS-dependent regulation in *S. meliloti* (19), and in *A. tumefaciens*, opines act as the conjugal signal for octopine-type Ti plasmids. Furthermore, in *A. tumefaciens* the octopine catabolic pathway and QS signal pathways are directly linked and *traR* is activated only when a threshold level of octopine is reached (95–97). The observation that the presence of AI represses rhizopine degradation in NGR234 might suggest, similarly to the *A. tumefaciens* system, a link between rhizopine metabolism and QS. In fact, He and colleagues (14) have previously suggested that rhizopines interfere with the regulation of *TraR* in NGR234. Thus, our observations are well in line with the hypothesis of He and colleagues.

Conclusions. Within this work, we have identified a set of 186 QS-regulated (*traI* and *ngrI*) genes in NGR234 using RNA-seq. We have provided evidence that the T3SS-II, T4P, biotin biosynthesis, and PQQ genes are QS regulated under the control of the *NgrI/R* regulon. These genes were so far not identified to be QS regulated in any of the other rhizobial model organisms. Our data further suggested that, similarly to *S. meliloti*, genes for flagellar and EPS (succinoglycan) biosynthesis are subject to QS-dependent regulation. While in general it is assumed that a homoge-

neous expression of these genes occurred throughout an isogenic population, there is now initial evidence that this may not be the natural situation. Instead, a fraction of the NGR234 genes are most likely heterogeneously expressed on a single-cell level (98). In the light of these novel findings, future work will now have to elucidate the complex pattern of gene expression and regulation on a single-cell level in this fascinating microorganism.

ACKNOWLEDGMENTS

This work was kindly funded by the German Federal Ministry of Education and Research (BMBF) within the framework of the ChemBiofilm network project and by the Deutsche Forschungsgemeinschaft through grant STR451/7-1 within the SPP1617 priority program.

We thank A. Jordan for help with the cloning and TLC assays.

REFERENCES

1. Waters CM, Bassler BL. 2005. Quorum sensing: cell-to-cell communication in bacteria. *Annu. Rev. Cell Dev. Biol.* 21:319–346. <http://dx.doi.org/10.1146/annurev.cellbio.21.012704.131001>.
2. Ng WL, Bassler BL. 2009. Bacterial quorum-sensing network architectures. *Annu. Rev. Genet.* 43:197–222. <http://dx.doi.org/10.1146/annurev-genet-102108-134304>.
3. Shank EA, Kolter R. 2009. New developments in microbial interspecies signaling. *Curr. Opin. Microbiol.* 12:205–214. <http://dx.doi.org/10.1016/j.mib.2009.01.003>.
4. de Kievit TR, Iglewski BH. 2000. Bacterial quorum sensing in pathogenic relationships. *Infect. Immun.* 68:4839–4849. <http://dx.doi.org/10.1128/IAI.68.9.4839-4849.2000>.
5. Val DL, Cronan JE, Jr. 1998. In vivo evidence that S-adenosylmethionine and fatty acid synthesis intermediates are the substrates for the LuxI family of autoinducer synthases. *J. Bacteriol.* 180:2644–2651.
6. Zeng LR, Xie JP. 2011. Molecular basis underlying LuxR family transcription factors and function diversity and implications for novel antibiotic drug targets. *J. Cell. Biochem.* 112:3079–3084. <http://dx.doi.org/10.1002/jcb.23262>.
7. Gage DJ. 2004. Infection and invasion of roots by symbiotic, nitrogen-fixing rhizobia during nodulation of temperate legumes. *Microbiol. Mol. Biol. Rev.* 68:280–300. <http://dx.doi.org/10.1128/MMBR.68.2.280-300.2004>.

8. Deakin WJ, Broughton WJ. 2009. Symbiotic use of pathogenic strategies: rhizobial protein secretion systems. *Nat. Rev. Microbiol.* 7:312–320. <http://dx.doi.org/10.1038/nrmicro2091>.
9. Jones KM, Kobayashi H, Davies BW, Taga ME, Walker GC. 2007. How rhizobial symbionts invade plants: the *Sinorhizobium-Medicago* model. *Nat. Rev. Microbiol.* 5:619–633. <http://dx.doi.org/10.1038/nrmicro1705>.
10. Broughton WJ, Perret X. 1999. Genealogy of legume-Rhizobium symbioses. *Curr. Opin. Plant Biol.* 2:305–311. [http://dx.doi.org/10.1016/S1369-5266\(99\)80054-5](http://dx.doi.org/10.1016/S1369-5266(99)80054-5).
11. Pueppke SG, Broughton WJ. 1999. *Rhizobium* sp. strain NGR234 and *R. fredii* USDA257 share exceptionally broad, nested host ranges. *Mol. Plant Microbe Interact.* 12:293–318. <http://dx.doi.org/10.1094/MPMI.1999.12.4.293>.
12. Trinick MJ. 1980. Relationships amongst the fast-growing rhizobia of *Lablab purpureus*, *Leucaena leucocephala*, *Mimosa* spp., *Acacia farnesiana* and *Sesbania grandiflora* and their affinities with other rhizobial groups. *J. Appl. Microbiol.* 49:39–53.
13. Schmeisser C, Liesegang H, Krysiak D, Bakkou N, Le Quere A, Wollherr A, Heinemeyer I, Morgenstern B, Pommerening-Röser A, Flores M, Palacios R, Brenner S, Gottschalk G, Schmitz RA, Broughton WJ, Perret X, Strittmatter AW, Streit WR. 2009. *Rhizobium* sp. strain NGR234 possesses a remarkable number of secretion systems. *Appl. Environ. Microbiol.* 75:4035–4045. <http://dx.doi.org/10.1128/AEM.00515-09>.
14. He X, Chang W, Pierce DL, Seib LO, Wagner J, Fuqua C. 2003. Quorum sensing in *Rhizobium* sp. strain NGR234 regulates conjugal transfer (*tra*) gene expression and influences growth rate. *J. Bacteriol.* 185:809–822. <http://dx.doi.org/10.1128/JB.185.3.809-822.2003>.
15. Marketon MM, González JE. 2002. Identification of two quorum-sensing systems in *Sinorhizobium meliloti*. *J. Bacteriol.* 184:3466–3475. <http://dx.doi.org/10.1128/JB.184.13.3466-3475.2002>.
16. Hoang HH, Becker A, González JE. 2004. The LuxR homolog ExpR, in combination with the Sin quorum sensing system, plays a central role in *Sinorhizobium meliloti* gene expression. *J. Bacteriol.* 186:5460–5472. <http://dx.doi.org/10.1128/JB.186.16.5460-5472.2004>.
17. Becker A, Bergès H, Krol E, Bruand C, Rüberg S, Capela D, Lauber E, Meilhoc E, Ampe F, de Bruijn FJ, Fourment J, Francez-Charlot A, Kahn D, Küster H, Liebe C, Pühler A, Weidner S, Batut J. 2004. Global changes in gene expression in *Sinorhizobium meliloti* 1021 under microoxic and symbiotic conditions. *Mol. Plant Microbe Interact.* 17:292–303. <http://dx.doi.org/10.1094/MPMI.2004.17.3.292>.
18. Gurich N, González JE. 2009. Role of quorum sensing in *Sinorhizobium meliloti*-alfalfa symbiosis. *J. Bacteriol.* 191:4372–4382. <http://dx.doi.org/10.1128/JB.00376-09>.
19. Gao M, Chen H, Eberhard A, Gronquist MR, Robinson JB, Rolfe BG, Bauer WD. 2005. *sinI*- and *expR*-dependent quorum sensing in *Sinorhizobium meliloti*. *J. Bacteriol.* 187:7931–7944. <http://dx.doi.org/10.1128/JB.187.23.7931-7944.2005>.
20. Chen H, Teplitski M, Robinson JB, Rolfe BG, Bauer WD. 2003. Proteomic analysis of wild-type *Sinorhizobium meliloti* responses to *N*-acyl homoserine lactone quorum-sensing signals and the transition to stationary phase. *J. Bacteriol.* 185:5029–5036. <http://dx.doi.org/10.1128/JB.185.17.5029-5036.2003>.
21. Charoenpanich P, Meyer S, Becker A, McIntosh M. 2013. Temporal expression program of quorum sensing-based transcription regulation in *Sinorhizobium meliloti*. *J. Bacteriol.* 195:3224–3236. <http://dx.doi.org/10.1128/JB.00234-13>.
22. Croucher NJ, Thomson NR. 2010. Studying bacterial transcriptomes using RNA-seq. *Curr. Opin. Microbiol.* 13:619–624. <http://dx.doi.org/10.1016/j.mib.2010.09.009>.
23. Haas BJ, Chin M, Nusbaum C, Birren BW, Livny J. 2012. How deep is deep enough for RNA-Seq profiling of bacterial transcriptomes? *BMC Genomics* 13:734. <http://dx.doi.org/10.1186/1471-2164-13-734>.
24. Sharma CM, Hoffmann S, Darfeuille F, Reignier J, Findeiss S, Sittka A, Chabas S, Reiche K, Hacker Müller J, Reinhardt R, Stadler PF, Vogel J. 2010. The primary transcriptome of the major human pathogen *Helicobacter pylori*. *Nature* 464:250–255. <http://dx.doi.org/10.1038/nature08756>.
25. Westermann AJ, Gorski SA, Vogel J. 2012. Dual RNA-seq of pathogen and host. *Nat. Rev. Microbiol.* 10:618–630. <http://dx.doi.org/10.1038/nrmicro2852>.
26. Schmid N, Pessi G, Deng Y, Aguilar C, Carlier AL, Grunau A, Omasits U, Zhang LH, Ahrens CH, Eberl L. 2012. The AHL- and BDSF-dependent quorum sensing systems control specific and overlapping sets of genes in *Burkholderia cenocepacia* H111. *PLoS One* 7:e49966. <http://dx.doi.org/10.1371/journal.pone.0049966>.
27. Chugani SA, Kim BS, Phattarasukol S, Brittnacher MJ, Choi SH, Harwood CS, Greenberg EP. 2012. Strain-dependent diversity in the *Pseudomonas aeruginosa* quorum-sensing regulon. *Proc. Natl. Acad. Sci. U. S. A.* 109:E2823–2831. <http://dx.doi.org/10.1073/pnas.1214128109>.
28. Wang D, Seeve C, Pierson L, Pierson E. 2013. Transcriptome profiling reveals links between ParS/ParR, MexEF-OprN, and quorum sensing in the regulation of adaptation and virulence in *Pseudomonas aeruginosa*. *BMC Genomics* 14:618. <http://dx.doi.org/10.1186/1471-2164-14-618>.
29. Li Y, Tian CF, Chen WF, Wang L, Sui XH, Chen WX. 2013. High-resolution transcriptomic analyses of *Sinorhizobium* sp. NGR234 bacteroids in determinate nodules of *Vigna unguiculata* and indeterminate nodules of *Leucaena leucocephala*. *PLoS One* 8:e70531. <http://dx.doi.org/10.1371/journal.pone.0070531>.
30. Fuqua C, Winans SC. 1996. Conserved *cis*-acting promoter elements are required for density-dependent transcription of *Agrobacterium tumefaciens* conjugal transfer genes. *J. Bacteriol.* 178:435–440.
31. Tempe J, Petit A, Holsters M, Montagu M, Schell J. 1977. Thermosensitive step associated with transfer of the Ti plasmid during conjugation: possible relation to transformation in crown gall. *Proc. Natl. Acad. Sci. U. S. A.* 74:2848–2849. <http://dx.doi.org/10.1073/pnas.74.7.2848>.
32. Sambrook J, Russell DW. 2001. Molecular cloning: a laboratory manual, 3rd ed. Cold Spring Harbor Laboratory Press, Cold Spring Harbor, NY.
33. Hornung C, Poehlein A, Haack FS, Schmidt M, Dierking K, Pohlen A, Schulenburg H, Blokesch M, Plener L, Jung K, Bonge A, Krohn-Molt I, Utpatel C, Timmermann G, Spieck E, Pommerening-Röser A, Bode E, Bode HB, Daniel R, Schmeisser C, Streit WR. 2013. The *Janthinobacterium* sp. HH01 genome encodes a homologue of the *V. cholerae* CqsA and *L. pneumophila* LqsA autoinducer synthases. *PLoS One* 8:e55045. <http://dx.doi.org/10.1371/journal.pone.0055045>.
34. Lassak J, Henche AL, Binnenkade L, Thormann KM. 2010. ArcS, the cognate sensor kinase in an atypical Arc system of *Shewanella oneidensis* MR-1. *Appl. Environ. Microbiol.* 76:3263–3274. <http://dx.doi.org/10.1128/AEM.00512-10>.
35. Kovach ME, Elzer PH, Hill DS, Robertson GT, Farris MA, Roop RM, II, Peterson KM. 1995. Four new derivatives of the broad-host-range cloning vector pBBR1MCS, carrying different antibiotic-resistance cassettes. *Gene* 166:175–176. [http://dx.doi.org/10.1016/0378-1119\(95\)00584-1](http://dx.doi.org/10.1016/0378-1119(95)00584-1).
36. Zhu J, Beaver JW, More MI, Fuqua WC, Eberhard A, Winans SC. 1998. Analogs of the autoinducer 3-oxooctanoyl-homoserine lactone strongly inhibit activity of the TraR protein of *Agrobacterium tumefaciens*. *J. Bacteriol.* 180:5398–5405.
37. Blomberg P, Wagner EG, Nordström K. 1990. Control of replication of plasmid R1: the duplex between the antisense RNA, CopA, and its target, CopT, is processed specifically *in vivo* and *in vitro* by RNase III. *EMBO J.* 9:2331–2340.
38. Dugar G, Herbig A, Förstner KU, Heidrich N, Reinhardt R, Nieselt K, Sharma CM. 2013. High-resolution transcriptome maps reveal strain-specific regulatory features of multiple *Campylobacter jejuni* isolates. *PLoS Genet.* 9:e1003495. <http://dx.doi.org/10.1371/journal.pgen.1003495>.
39. Hoffmann S, Otto C, Kurtz S, Sharma CM, Khativich P, Vogel J, Stadler PF, Hacker Müller J. 2009. Fast mapping of short sequences with mismatches, insertions and deletions using index structures. *PLoS Comput. Biol.* 5:e1000502. <http://dx.doi.org/10.1371/journal.pcbi.1000502>.
40. Nicol JW, Helt GA, Blanchard SG, Jr, Raja A, Loraine AE. 2009. The Integrated Genome Browser: free software for distribution and exploration of genome-scale datasets. *Bioinformatics* 25:2730–2731. <http://dx.doi.org/10.1093/bioinformatics/btp472>.
41. Rivas R, Vizcaíno N, Buey RM, Mateos PF, Martínez-Molina E, Velázquez E. 2001. An effective, rapid and simple method for total RNA extraction from bacteria and yeast. *J. Microbiol. Methods* 47:59–63. [http://dx.doi.org/10.1016/S0167-7012\(01\)00292-5](http://dx.doi.org/10.1016/S0167-7012(01)00292-5).
42. Krishnan HB, Pueppke SG. 1991. Sequence and analysis of the *nodABC* region of *Rhizobium fredii* USDA257, a nitrogen-fixing symbiont of soybean and other legumes. *Mol. Plant Microbe Interact.* 4:512–520. <http://dx.doi.org/10.1094/MPMI-4-512>.
43. Edgar R, Domrachev M, Lash AE. 2002. Gene Expression Omnibus: NCBI gene expression and hybridization array data repository. *Nucleic Acids Res.* 30:207–210. <http://dx.doi.org/10.1093/nar/30.1.207>.
44. Dötsch A, Eckweiler D, Schniederjans M, Zimmermann A, Jensen V, Scharfe M, Geffers R, Häussler S. 2012. The *Pseudomonas aeruginosa*

- transcriptome in planktonic cultures and static biofilms using RNA sequencing. *PLoS One* 7:e31092. <http://dx.doi.org/10.1371/journal.pone.0031092>.
45. Georg J, Hess WR. 2011. *cis*-antisense RNA, another level of gene regulation in bacteria. *Microbiol. Mol. Biol. Rev.* 75:286–300. <http://dx.doi.org/10.1128/MMBR.00032-10>.
 46. Lasa I, Toledo-Arana A, Gingeras TR. 2012. An effort to make sense of antisense transcription in bacteria. *RNA Biol.* 9:1039–1044. <http://dx.doi.org/10.4161/rna.21167>.
 47. Wagner VE, Bushnell D, Passador L, Brooks AI, Iglewski BH. 2003. Microarray analysis of *Pseudomonas aeruginosa* quorum-sensing regulators: effects of growth phase and environment. *J. Bacteriol.* 185:2080–2095. <http://dx.doi.org/10.1128/JB.185.7.2080-2095.2003>.
 48. Schuster M, Lostroh CP, Ogi T, Greenberg EP. 2003. Identification, timing, and signal specificity of *Pseudomonas aeruginosa* quorum-controlled genes: a transcriptome analysis. *J. Bacteriol.* 185:2066–2079. <http://dx.doi.org/10.1128/JB.185.7.2066-2079.2003>.
 49. Hentzer M, Wu H, Andersen JB, Riedel K, Rasmussen TB, Bagge N, Kumar N, Schembri MA, Song Z, Kristoffersen P, Manefield M, Costerton JW, Molin S, Eberl L, Steinberg P, Kjelleberg S, Høiby N, Givskov M. 2003. Attenuation of *Pseudomonas aeruginosa* virulence by quorum sensing inhibitors. *EMBO J.* 22:3803–3815. <http://dx.doi.org/10.1093/emboj/cdg366>.
 50. Bijtenhoorn P, Mayerhofer H, Müller-Dieckmann J, Utpatel C, Schipper C, Hornung C, Szesny M, Grond S, Thürmer A, Brzuszkiewicz E, Daniel R, Dierking K, Schulenburg H, Streit WR. 2011. A novel meta-genomic short-chain dehydrogenase/reductase attenuates *Pseudomonas aeruginosa* biofilm formation and virulence on *Caenorhabditis elegans*. *PLoS One* 6:e26278. <http://dx.doi.org/10.1371/journal.pone.0026278>.
 51. LaRock CN, Yu J, Horswill AR, Parsek MR, Minion FC. 2013. Transcriptome analysis of acetyl-homoserine lactone-based quorum sensing regulation in *Yersinia pestis*. *PLoS One* 8:e62337. <http://dx.doi.org/10.1371/journal.pone.0062337>.
 52. Parkhill J, Wren BW, Thomson NR, Titball RW, Holden MT, Prentice MB, Sebahia M, James KD, Churcher C, Mungall KL, Baker S, Basham D, Bentley SD, Brooks K, Cerdeño-Tárraga AM, Chillingworth T, Cronin A, Davies RM, Davis P, Dougan G, Feltwell T, Hamlin N, Holroyd S, Jagels K, Karlyshev AV, Leather S, Moulé S, Oyston PC, Quail M, Rutherford K, Simmonds M, Skelton J, Stevens K, Whitehead S, Barrell BG. 2001. Genome sequence of *Yersinia pestis*, the causative agent of plague. *Nature* 413:523–527. <http://dx.doi.org/10.1038/35097083>.
 53. Daniels R, De Vos DE, Desair J, Raedschelders G, Luyten E, Rosemeyer V, Verreth C, Schoeters E, Vanderleyden J, Michiels J. 2002. The *cin* quorum sensing locus of *Rhizobium etli* CNPAF512 affects growth and symbiotic nitrogen fixation. *J. Biol. Chem.* 277:462–468. <http://dx.doi.org/10.1074/jbc.M106655200>.
 54. Gray KM, Pearson JP, Downie JA, Boboye BE, Greenberg EP. 1996. Cell-to-cell signaling in the symbiotic nitrogen-fixing bacterium *Rhizobium leguminosarum*: autoinduction of a stationary phase and rhizosphere-expressed genes. *J. Bacteriol.* 178:372–376.
 55. Krysciak D, Schmeisser C, Preuss S, Riethausen J, Quitschau M, Grond S, Streit WR. 2011. Involvement of multiple loci in quorum quenching of autoinducer I molecules in the nitrogen-fixing symbiont *Rhizobium (Sinorhizobium)* sp. strain NGR234. *Appl. Environ. Microbiol.* 77:5089–5099. <http://dx.doi.org/10.1128/AEM.00112-11>.
 56. Fujishige NA, Kapadia NN, De Hoff PL, Hirsch AM. 2006. Investigations of *Rhizobium* biofilm formation. *FEMS Microbiol. Ecol.* 56:195–206. <http://dx.doi.org/10.1111/j.1574-6941.2005.00044.x>.
 57. Kape R, Parniske M, Werner D. 1991. Chemotaxis and *nod* gene activity of *Bradyrhizobium japonicum* in response to hydroxycinnamic acids and isoflavonoids. *Appl. Environ. Microbiol.* 57:316–319.
 58. Finan TM, Gough C, Truchet G. 1995. Similarity between the *Rhizobium meliloti* *fliP* gene and pathogenicity-associated genes from animal and plant pathogens. *Gene* 152:65–67. [http://dx.doi.org/10.1016/0378-1119\(94\)00643-7](http://dx.doi.org/10.1016/0378-1119(94)00643-7).
 59. Ames P, Bergman K. 1981. Competitive advantage provided by bacterial motility in the formation of nodules by *Rhizobium meliloti*. *J. Bacteriol.* 148:728–729.
 60. Gao M, Coggin A, Yagnik K, Teplitski M. 2012. Role of specific quorum-sensing signals in the regulation of exopolysaccharide II production within *Sinorhizobium meliloti* spreading colonies. *PLoS One* 7:e42611. <http://dx.doi.org/10.1371/journal.pone.0042611>.
 61. Hoang HH, Gurich N, González JE. 2008. Regulation of motility by the *ExpR/Sin* quorum-sensing system in *Sinorhizobium meliloti*. *J. Bacteriol.* 190:861–871. <http://dx.doi.org/10.1128/JB.01310-07>.
 62. Shi W, Sun H. 2002. Type IV pilus-dependent motility and its possible role in bacterial pathogenesis. *Infect. Immun.* 70:1–4. <http://dx.doi.org/10.1128/IAI.70.1.1-4.2002>.
 63. Vesper SJ, Bauer WD. 1986. Role of pili (fimbriae) in attachment of *Bradyrhizobium japonicum* to soybean roots. *Appl. Environ. Microbiol.* 52:134–141.
 64. Barken KB, Pamp SJ, Yang L, Gjermansen M, Bertrand JJ, Klausen M, Givskov M, Whitchurch CB, Engel JN, Tolker-Nielsen T. 2008. Roles of type IV pili, flagellum-mediated motility and extracellular DNA in the formation of mature multicellular structures in *Pseudomonas aeruginosa* biofilms. *Environ. Microbiol.* 10:2331–2343. <http://dx.doi.org/10.1111/j.1462-2920.2008.01658.x>.
 65. Skorupska A, Janczarek M, Marczak M, Mazur A, Król J. 2006. Rhizobial exopolysaccharides: genetic control and symbiotic functions. *Microb. Cell Fact.* 5:7. <http://dx.doi.org/10.1186/1475-2859-5-7>.
 66. Le Quere AJ, Deakin WJ, Schmeisser C, Carlson RW, Streit WR, Broughton WJ, Forsberg LS. 2006. Structural characterization of a K-antigen capsular polysaccharide essential for normal symbiotic infection in *Rhizobium* sp. NGR234: deletion of the *rkpMNO* locus prevents synthesis of 5,7-diacetamido-3,5,7,9-tetra-deoxy-non-2-ulosonic acid. *J. Biol. Chem.* 281:28981–28992.
 67. Streit WR, Schmitz RA, Perret X, Staehelin C, Deakin WJ, Raasch C, Liesegang H, Broughton WJ. 2004. An evolutionary hot spot: the pNGR234b replicon of *Rhizobium* sp. strain NGR234. *J. Bacteriol.* 186:535–542. <http://dx.doi.org/10.1128/JB.186.2.535-542.2004>.
 68. Staehelin C, Forsberg LS, D’Haeze W, Gao MY, Carlson RW, Xie ZP, Pellock BJ, Jones KM, Walker GC, Streit WR, Broughton WJ. 2006. Exo-oligosaccharides of *Rhizobium* sp. strain NGR234 are required for symbiosis with various legumes. *J. Bacteriol.* 188:6168–6178. <http://dx.doi.org/10.1128/JB.00365-06>.
 69. Chen H, Gray J, Nayudu M, Djordjevic M, Batley M, Redmond J, Rolfe B. 1988. Five genetic loci involved in the synthesis of acidic exopolysaccharides are closely linked in the genome of *Rhizobium* sp. strain NGR234. *Mol. Gen. Genet.* 212:310–316. <http://dx.doi.org/10.1007/BF00334701>.
 70. Glenn SA, Gurich N, Feeny MA, González JE. 2007. The *ExpR/Sin* quorum-sensing system controls succinoglycan production in *Sinorhizobium meliloti*. *J. Bacteriol.* 189:7077–7088. <http://dx.doi.org/10.1128/JB.00906-07>.
 71. Streit WR, Joseph CM, Phillips DA. 1996. Biotin and other water-soluble vitamins are key growth factors for alfalfa root colonization by *Rhizobium meliloti* 1021. *Mol. Plant Microbe Interact.* 9:330–338. <http://dx.doi.org/10.1094/MPMI-9-0330>.
 72. Hofmann K, Heinz EB, Charles TC, Hoppert M, Liebl W, Streit WR. 2000. *Sinorhizobium meliloti* strain 1021 *bioS* and *bdhA* gene transcriptions are both affected by biotin available in defined medium. *FEMS Microbiol. Lett.* 182:41–44. <http://dx.doi.org/10.1111/j.1574-6968.2000.tb08870.x>.
 73. Dunn MF, Encarnación S, Araiza G, Vargas MC, Dávalos A, Peralta H, Mora Y, Mora J. 1996. Pyruvate carboxylase from *Rhizobium etli*: mutant characterization, nucleotide sequence, and physiological role. *J. Bacteriol.* 178:5960–5970.
 74. Dunn MF. 2011. Anaplerotic function of phosphoenolpyruvate carboxylase in *Bradyrhizobium japonicum* USDA110. *Curr. Microbiol.* 62:1782–1788. <http://dx.doi.org/10.1007/s00284-011-9928-y>.
 75. Streit WR, Entcheva P. 2003. Biotin in microbes, the genes involved in its biosynthesis, its biochemical role and perspectives for biotechnological production. *Appl. Microbiol. Biotechnol.* 61:21–31. <http://dx.doi.org/10.1007/s00253-002-1186-2>.
 76. Heinz EB, Phillips DA, Streit WR. 1999. BioS, a biotin-induced, stationary-phase, and possible LysR-type regulator in *Sinorhizobium meliloti*. *Mol. Plant Microbe Interact.* 12:803–812. <http://dx.doi.org/10.1094/MPMI.1999.12.9.803>.
 77. Streit WR, Phillips DA. 1997. A biotin-regulated locus, *bioS*, in a possible survival operon of *Rhizobium meliloti*. *Mol. Plant Microbe Interact.* 10:933–937. <http://dx.doi.org/10.1094/MPMI.1997.10.7.933>.
 78. Goodwin PM, Anthony C. 1998. The biochemistry, physiology and genetics of PQQ and PQQ-containing enzymes. *Adv. Microb. Physiol.* 40:1–80. [http://dx.doi.org/10.1016/S0065-2911\(08\)60129-0](http://dx.doi.org/10.1016/S0065-2911(08)60129-0).
 79. Bernardelli CE, Luna MF, Galar ML, Boiardi JL. 2008. Symbiotic phenotype of a membrane-bound glucose dehydrogenase mutant of *Sinorhi-*

- zobium meliloti*. Plant Soil 313:217–225. <http://dx.doi.org/10.1007/s11104-008-9694-1>.
80. Bernardelli CE, Luna MF, Galar ML, Boiardi JL. 2001. Periplasmic PQQ-dependent glucose oxidation in free-living and symbiotic rhizobia. Curr. Microbiol. 42:310–315. <http://dx.doi.org/10.1007/s002840010222>.
 81. Sandkvist M. 2001. Biology of type II secretion. Mol. Microbiol. 40:271–283. <http://dx.doi.org/10.1046/j.1365-2958.2001.02403.x>.
 82. Coburn B, Sekirov I, Finlay BB. 2007. Type III secretion systems and disease. Clin. Microbiol. Rev. 20:535–549. <http://dx.doi.org/10.1128/CMR.00013-07>.
 83. Freiberg C, Fellay R, Bairoch A, Broughton WJ, Rosenthal A, Perret X. 1997. Molecular basis of symbiosis between *Rhizobium* and legumes. Nature 387:394–401. <http://dx.doi.org/10.1038/387394a0>.
 84. Ausmees N, Kobayashi H, Deakin WJ, Marie C, Krishnan HB, Broughton WJ, Perret X. 2004. Characterization of NopP, a type III secreted effector of *Rhizobium* sp. strain NGR234. J. Bacteriol. 186:4774–4780. <http://dx.doi.org/10.1128/JB.186.14.4774-4780.2004>.
 85. Viprey V, Del Greco A, Golinowski W, Broughton WJ, Perret X. 1998. Symbiotic implications of type III protein secretion machinery in *Rhizobium*. Mol. Microbiol. 28:1381–1389. <http://dx.doi.org/10.1046/j.1365-2958.1998.00920.x>.
 86. Marie C, Deakin WJ, Ojanen-Reuhs T, Diallo E, Reuhs B, Broughton WJ, Perret X. 2004. TtsI, a key regulator of *Rhizobium* species NGR234 is required for type III-dependent protein secretion and synthesis of rhamnose-rich polysaccharides. Mol. Plant Microbe Interact. 17:958–966. <http://dx.doi.org/10.1094/MPMI.2004.17.9.958>.
 87. Kobayashi H, Naciri-Graven Y, Broughton WJ, Perret X. 2004. Flavonoids induce temporal shifts in gene-expression of *nod*-box controlled loci in *Rhizobium* sp. NGR234. Mol. Microbiol. 51:335–347. <http://dx.doi.org/10.1046/j.1365-2958.2003.03841.x>.
 88. Bakkou N, Perret X. 2008. Functional analysis of a second type III secretion system in *Rhizobium* sp. NGR234, p 209. In Holsters M (ed), Abstr. 8th Eur. Nitrogen Fixation Conf., Ghent, Belgium.
 89. Chugani SA, Whiteley M, Lee KM, D'Argenio D, Manoel C, Greenberg EP. 2001. QscR, a modulator of quorum-sensing signal synthesis and virulence in *Pseudomonas aeruginosa*. Proc. Natl. Acad. Sci. U. S. A. 98:2752–2757. <http://dx.doi.org/10.1073/pnas.051624298>.
 90. Seet Q, Zhang LH. 2011. Anti-activator QslA defines the quorum sensing threshold and response in *Pseudomonas aeruginosa*. Mol. Microbiol. 80:951–965. <http://dx.doi.org/10.1111/j.1365-2958.2011.07622.x>.
 91. Murphy PJ, Heycke N, Banfalvi Z, Tate ME, de Bruijn FJ, Kondorosi A, Tempe J, Schell J. 1987. Genes for the catabolism and synthesis of an opine-like compound in *Rhizobium meliloti* are closely linked and on the Sym plasmid. Proc. Natl. Acad. Sci. U. S. A. 84:493–497. <http://dx.doi.org/10.1073/pnas.84.2.493>.
 92. Saint CP, Wexler M, Murphy PJ, Tempe J, Tate ME, Murphy PJ. 1993. Characterization of genes for synthesis and catabolism of a new rhizopine induced in nodules by *Rhizobium meliloti* Rm220-3: extension of the rhizopine concept. J. Bacteriol. 175:5205–5215.
 93. Rossbach S, Rasul G, Schneider M, Eardly B, de Bruijn FJ. 1995. Structural and functional conservation of the rhizopine catabolism (*moc*) locus is limited to selected *Rhizobium meliloti* strains and unrelated to their geographical origin. Mol. Plant Microbe Interact. 8:549–559. <http://dx.doi.org/10.1094/MPMI-8-0549>.
 94. Kohler PR, Zheng JY, Schoffers E, Rossbach S. 2010. Inositol catabolism, a key pathway in *Sinorhizobium meliloti* for competitive host nodulation. Appl. Environ. Microbiol. 76:7972–7980. <http://dx.doi.org/10.1128/AEM.01972-10>.
 95. Oger P, Kim K-S, Sackett RL, Piper KR, Farrand SK. 1998. Octopine-type Ti plasmids code for a mannopine-inducible dominant-negative allele of *traR*, the quorum-sensing activator that regulates Ti plasmid conjugal transfer. Mol. Microbiol. 27:277–288. <http://dx.doi.org/10.1046/j.1365-2958.1998.00671.x>.
 96. Fuqua C, Burbea M, Winans SC. 1995. Activity of the *Agrobacterium* Ti plasmid conjugal transfer regulator TraR is inhibited by the product of the *traM* gene. J. Bacteriol. 177:1367–1373.
 97. Fuqua C, Winans SC. 1996. Localization of OccR-activated and TraR-activated promoters that express two ABC-type permeases and the *traR* gene of Ti plasmid pTiR10. Mol. Microbiol. 20:1199–1210. <http://dx.doi.org/10.1111/j.1365-2958.1996.tb02640.x>.
 98. Grote J, Krysciak D, Schorn A, Dahlke RL, Soonvald L, Müller J, Hense BA, Schwarzfischer M, Sauter M, Schmeisser C, Streit WR. 2014. Evidence of autoinducer-dependent and -independent heterogeneous gene expression in *Sinorhizobium fredii* NGR234. Appl. Environ. Microbiol. 80:5572–5582. <http://dx.doi.org/10.1128/AEM.01689-14>.
 99. Krzywinski MI, Schein JE, Birol I, Connors J, Gascoyne R, Horsman D, Jones SJ, Marra MA. 2009. Circos: an information aesthetic for comparative genomics. Genome Res. 19:1639–1645. <http://dx.doi.org/10.1101/gr.092759.109>.